Effects of Galvanizing on Residual Stresses and Stress Concentrations in RHS X- and T-Connections

by

Ye Jin

A Thesis Submitted in Partial Fulfillment of the
Requirements for the Degree of

Master of Applied Science

in the Department of Civil Engineering

University of Victoria

Effects of Galvanizing on Residual Stresses and Stress Concentrations in RHS X- and T-Connections

by

Ye Jin

Supervisory Committee:

Dr. Min Sun, Supervisor
Department of Civil Engineering

Dr. Cheng Lin, Departmental Member
Department of Civil Engineering

Abstract

Complementary studies showed that post-production hot-dip galvanizing changes residual stress magnitudes and distributions in cold-formed hollow structural section (HSS) members and can affect their behaviours under axial compressive and flexural loads. However, research on the effects of galvanizing on HSS connections is insufficient. Similar to previous research, in this research, a comprehensive measurement of residual stresses was performed, using the hole-drilling approach and a total of 144 strain gauge elements at 48 locations of interest on the connection specimens. The experimental program includes two galvanized and two ungalvanized rectangular hollow section (RHS) connection specimens with different branch-to-chord width ratios (β). The effects of fabrication (cold forming and welding) and post-fabrication (galvanizing) processes on residual stresses at various locations of the specimens are investigated and compared. The effects of galvanizing-induced residual stress changes on stress concentrations at the critical locations at different fatigue load levels are studied. The connection specimens were subsequently tested under branch axial compressive forces to failure to compare their performances under static loading.

Keywords: Rectangular Hollow Section; Hollow Structural Section; tubular connection; galvanizing; residual stress; stress concentration; hot spot stress; fatigue design.

Table of Contents

Supervisory Committee: ..... **ii**

Abstract ..... **iii**

Table of Contents ..... **iv**

List of Tables ..... **vi**

List of Figures ..... **vii**

Acknowledgements ..... **viii**

Nomenclature ..... **ix**

Chapter 1. Introduction **1**

Chapter 2. Review of relevant research and design recommendations **3**

Chapter 3. Experimental program **7**

3.1. Connection specimens 7

3.2. Material properties 8

3.3. Setup for measurements 9

3.4. Locations of strain gauge rosettes 11

3.5. Residual stresses calculation 14

Chapter 4. Experimental results and discussions **17**

4.1. Summary 17

4.2. Effects of cold forming 22

4.3. Effects of welding 23

4.4. Effects of galvanizing 24

Chapter 5. Stress concentrations at different fatigue load levels **25**

5.1. Summary 25

5.2. Effects of load level and galvanizing 27

5.3. Effects of load level, joint fabrication and galvanizing 29

Chapter 6. Testing of connection specimens under quasi-static branch axial loads 32

6.1. Test setup and instrumentation 32

6.2. Failure modes 34

6.3. Test results 34

6.4. Discussions of connection test results 37

Chapter 7. Conclusions 38

Appendix I. Coupon test results 39

Appendix II. Type A strain gauge rosettes parameters 41

Appendix III. Residual stress test results 42

Appendix IV. References 45

List of Tables

Table 1. Measured residual stresses in tubular steel connections and members from previous studies 4

Table 2. Nominal dimensions of connection specimens 8

Table 3. Primary sources of residual stresses in connection specimens 14

Table 4. Stress concentration factors calculated using CIDEC Design Guide 8 rules 27

Table I.1. Tensile coupon test results 40

Table II.1. Type A strain gauge rosette parameters 41

Table II.2. Uniform residual stress evaluation coefficients 41

Table III.1. Residual stresses calculation results 42

Table III.2. Residual stresses perpendicular to weld toes 44

List of Figures

Figure 1. Galvanizing of rectangular hollow section truss 2

Figure 2. Typical connection specimen and symbol definitions 8

Figure 3. Equipment and setup recommended by ASTM E837 for aliment and residual stress measurement 10

Figure 4. Typical connection specimen after branch cutting 10

Figure 5. Hot spot locations recommended by CIDECT Design Guide 8 12

Figure 6. Locations of strain gauge rosettes on X-0.5 and GX-0.5 13

Figure 7. Residual stresses in X-0.5 18

Figure 8. Residual stresses in X-0.7 19

Figure 9. Residual stresses in GX-0.5 20

Figure 10. Residual stresses in GX-0.7 21

Figure 11. Residual stresses perpendicular to weld toe 26

Figure 12. Residual stress factor (RSF) distributions for hot spot locations in Fig. 5 28

Figure 13. Residual stress correction factor (ψ) distributions for hot spot locations in Fig. 5 31

Figure 14. Typical test setup 32

Figure 15. Locations of Linear Variable Differential Transformers (LVDTs) 33

Figure 16. Load-displacement curves 35

Figure 17. Typical failure mode 35

Figure 18. Chord face deformation profiles 36

Figure I.1. Tensile coupon stress-strain curves with the 0.2% offset yield strength 39

Figure I.2. Tensile coupons after test 40

Figure II.1. Typical type A strain gauge rosette 41

Acknowledgements

I am grateful for the financial support from the Natural Sciences and Engineering Research Council of Canada (NSERC) and the British Columbia Institute of Technology (BCIT).

I would like to express my deepest gratitude to my program supervisor Professor Min Sun, for his invaluable guidance, encouragement, and support throughout my research journey. His expertise and insights are invaluable resources.

I also want to extend my heartfelt thanks to Dr. Armando Tura, Bastien Lanusse and Solomon Rosenberg from University of Victoria Civil Engineering Laboratory and Ray Daxon from BCIT Structures Lab for their support and assistance. I am grateful for the opportunity to work with such talented and dedicated teams.

Finally, I want to thank my family for their love and support throughout this process. Their encouragement and belief in me have been a constant source of motivation and inspiration.

Nomenclature

E	Young's modulus
f_y	yield stress
f_u	ultimate stress
N_1	branch axial load
$N_{1,u}$	maximum branch axial load
$N_{1,3\%}$	connection load at an ultimate deformation of 3% b_0
RSF	residual stress factor
SCF_A	branch SCF at hot spot A
SCF_B	chord SCF at hot spot B
SCF_C	chord SCF at hot spot C
SCF_D	chord SCF at hot spot D
SCF_E	branch SCF at hot spot E
SCF_i	SCF at hot spot i in an RHS-to-RHS axially loaded X-connection
b_0	chord width
b_1	branch width
e	end distance = distance from the heel/toe of the closest branch to the chord end
h_0	chord height
h_1	branch height
i	parameter used to designate a critical (hot spot) location (i = A, B, C, D or E)
l_0	chord length
t_0	chord wall thickness
t_1	branch wall thickness
α	chord length parameter (= $2l_0/b_0$ or $2l_0/d_0$)
β	branch-to-chord width ratio (= b_1/b_0)
γ	half chord width-to-thickness ratio (= $b_0/2t_0$)
τ	branch-to-chord thickness ratio (= t_1/t_0)
θ	acute angle between the branch and chord (in degrees)
ψ	residual stress correction factor
σ_n	nominal stress
$\sigma_{rs,long}$	residual stress in chord longitudinal direction
$\sigma_{rs,p}$	maximum principal residual stress
$\sigma_{rs,tran}$	residual stress in chord transverse direction
$\Delta\sigma_{rs,fab,i}$	joint fabrication-induced residual stress change at hot spot i
$\Delta\sigma_{rs,gal,i}$	galvanizing-induced residual stress change at hot spot i

δ	vertical connection displacement
ε_{rup}	rupture strain

Chapter 1. Introduction

From power generation to transmission and distribution, many energy infrastructures are built with galvanized tubular steel structures. For transportation infrastructure, the application of galvanized tubular steel structures covers nearly all fields. Such infrastructure projects are long-term and costly investments. Design and fabrication of robust and durable energy infrastructure standing up to not only the static and fatigue loadings but also the harsh environment and test of time continue to be one of the largest challenges in the engineering community.

For hot-dip galvanizing, the molten zinc bath is typically maintained at 450°C. When galvanizing steel trusses of commonly specified sizes (Fig. 1), nearly the same steps are followed in all facilities. The immersion time for individual parts of a truss is strictly controlled (approximately five minutes for each connection) to produce the best coating quality [1-10]. For cold-formed hollow structural section (HSS), similar to the heat treatment (also at 450°C) per ASTM A1085 Supplement S1 [11], or the Class H finish per CSA G40.20/G40.21 [12], the galvanizing temperature has little effect on the material strength and ductility as a higher temperature is needed to produce metallurgical changes. However, this process inevitably changes the residual stress magnitudes and distributions in cold-formed HSS members [1-10]. To facilitate the application of galvanized high-strength HSS in infrastructure projects, recent research [2,6-10] showed that, for commonly specified cross-sectional sizes, similar to the heat treatment per ASTM A1085 [11] and CSA G40.20/G40.21 [12], hot-dip galvanizing can improve member behaviours under axial compressive and flexural loads through effective partial residual stress relief.

Similarly, it is speculated that hot-dip galvanizing will affect residual stresses in welded tubular steel connections and subsequently connection fatigue behaviours [1]. Since no definitive research on this topic is available to this day, this paper presents a comprehensive measurement of residual stresses using the hole-drilling method and a total of 144 strain gauge elements at different locations of interest on the connection specimens. This paper represents a first step towards understanding the effects of post-fabrication hot-dip galvanizing on residual stresses and stress concentrations in welded tubular steel connections. The experimental program includes two galvanized and two ungalvanized rectangular hollow section (RHS) connection

specimens. The overall approach is similar to previous research [13] on residual stresses in high-strength steel built-up connection (with and without heat treatment) where a comprehensive measurement was taken on two connection specimens at the critical locations around the welded joints. In this study, the effects of cold forming, welding and galvanizing on the residual stresses around the perimeters of the welded joints of the four connection specimens are investigated and compared. The effects of galvanizing-induced residual stress changes on local stress concentrations and connection fatigue resistances at different load levels are studied.

Fig. 1. Galvanizing of rectangular hollow section truss (Ford Pedestrian Bridge in Chicago, IL, United States) [Photo courtesy of American Galvanizers Association]

It is also speculated that galvanizing-induced residual stress changes may influence connection behaviour under static loading [1]. Therefore, after residual stress measurements, the four connection specimens are tested under quasi-static branch axial compression for further comparison and examination of the speculation.

Chapter 2. Review of relevant research and design recommendations

Residual stresses are inevitably generated in steel members and connections during fabrication (e.g., cold forming and welding) and post-fabrication (e.g., galvanizing) processes. Table 1 lists the key findings of representative previous research in this field. Table 1 covers galvanizing-induced residual stress changes in tubular steel members but not welded tubular steel connections since no definitive research on this topic is available to this day. However, the key findings of the listed research are valuable as they not only provide the basis for comparison but also substantiate the need for the connection research presented in this paper.

For commonly specified cross-sectional dimensions, RHS are internationally manufactured predominantly by two approaches: (1) "indirect forming" where the coil material is first cold formed to a circular shape and subsequently to the desired rectangular shape; and (2) "direct forming" where the coil material is directly cold formed to the desired rectangular shape. At the four flat faces, an indirect-formed section in general contains higher levels of residual stresses comparing to its direct-formed counterpart. On the other hand, the residual stresses produced by the two cold forming approaches at the four corner regions are in theory similar, as the bend radii are similar [7,15,17-19]. As shown by the representative studies [7,15] in Table 1, for both regular- and high-strength RHS, the residual stresses due to cold forming can be significant when compared to the material yield strengths. Detailed discussions on similar studies can be found in [7,15]. No attempt is made in this paper on a detailed review of all relevant studies.

Welding-induced residual stresses in the first few millimeters from the component surface [e.g., 13,14,16] are of particular interest to researchers since they affect the initiation and propagation of surface cracks at the weld toe under fatigue loading. [13] investigated the effects of welding-induced residual stresses on fatigue behaviour of built-up box T-connections. [14] investigated the effect of residual stress due to cold forming plus welding on fatigue behaviour of welded circular hollow section (CHS)-to-CHS K-connections. The key findings are summarized in Table 1. As shown, such residual stress can also be higher than 50% of the measured material yield strength, and in turn affect connection fatigue behaviour.

Table 1. Measured residual stresses in tubular steel connections and members from previous studies

Study	Yield strength	Primary source of residual stress	Key findings
Built-up box T-connections without preheating [13]	Nominal: 690 MPa Measured: 770 MPa	Welding	Residual stress on chord surface near branch corner: 200-415 MPa(1) Residual stress on chord surface near branch centerline: 85-250 MPa(1)
Built-up box T-connections with preheating [13]	Nominal: 690 Measured: 770	Welding, preheating	Residual stress on chord surface near branch corner: 100-350 MPa(1) Residual stress on chord surface near branch centerline: 10-120 MPa(1)
Circular hollow section K-connections [14]	Nominal: 355 MPa Measured: 430-630 MPa	Cold forming and welding	Residual stress on welded joint surface: 250-400 MPa(1)
RHS members (indirect- and direct-formed) [15]	Nominal: 235 and 345 MPa Measured: 257-404 MPa (from tensile testing of coupons from flat face)	Cold forming and welding	Proposed though-thickness longitudinal residual stress models. Flat face: up to 66% of measured yield strength Corner region: up to 58% of measured yield strength
Built-up box section members [16]	Nominal: 460 MPa Measured: 506 MPa	Welding	Measured residual stresses: 300-400 MPa(2)
RHS members (indirect- and direct-formed) [7]	Nominal: 350 MPa Measured: 367-483 MPa(3)	Cold forming	Average of bending residual stresses over entire cross-section: 62%-80% of measured yield strengths(4)
Galvanized RHS members (indirect- and direct-formed) [7]	Nominal: 350 MPa Measured: 367-483 MPa(3)	Cold forming and galvanizing	Average of bending residual stresses over entire cross-section: 33%-50% of measured yield strengths(4)
High-strength RHS members (direct-formed) [7]	Nominal: 690 MPa Measured: 638-730 MPa(3)	Cold forming	Average of bending residual stresses over entire cross-section: 49%-69% of measured yield strengths(4)
Galvanized high-strength RHS members (direct-formed) [7]	Nominal: 690 MPa Measured: 638-730 MPa(3)	Cold forming and galvanizing	Average of bending residual stresses over entire cross-section: 24%-37% of measured yield strengths(4)

(1) The residual stresses are measured on connection surface adjacent to weld seam, using the hole-drilling, X-ray diffraction or neutron diffraction approach.
(2) The residual stresses are measured using the hole-drilling and sectioning approaches. The listed values are from member surface.
(3) For direct comparison to [15], the listed values are the measured yield strengths from tensile testing of the flat face coupons from the parent materials prior to hot-dip galvanizing.
(4) The listed residual stress values are calculated based on measurements on member surfaces using the sectioning approach which assumes a linear through-thickness distribution.

For hot-dip galvanizing, the molten zinc bath is typically maintained at 450°C. When galvanizing steel trusses of commonly specified sizes (Fig. 1), nearly the same steps are followed in all facilities [1-5]. The

dipping and withdrawing rates are carefully controlled to ensure sufficient reactivity and in turn good coverage and quality of coating. On the other hand, an excessively long immersion time will result in an excessively thick zinc coating. Such coating is not economic and can be brittle due to the overreaction between the zinc bath and the base steel [1-10]. For unbraced thin-walled steel sections, the thermal effect of the hot dipping process can sometimes cause warpage and distortion [1]. Therefore, it is intuitive that galvanizing will affect the residual stress magnitudes and distributions in cold-formed HSS members and connections. Recent experimental research [7] has been performed to compare the residual stresses in regular- and high-strength RHS before and after hot-dip galvanizing and heat treatment. It was experimentally observed that the current industrial practice for hot-dip galvanizing can partially relieve residual stresses in cold-formed RHS. This can be seen by comparing the normalized ranges of residual stress from [7] in Table 1. For regular-strength RHS, the bending residual stresses changed from 62% - 80% of the measured yield stresses to 33% - 50%. For high-strength RHS, the bending residual stresses changed from 49% - 69% of the measured yield stresses to 24% - 37%. The level of relief is close to those from the heat treatment per ASTM A1085 Supplement S1 [11] and the Class H finish per CSA G40.20/G40.21 [12]. It should be noted that the ASTM A1085 and the CSA G40.20/G40.21 heat treatments (also at 450°C) justify the use of a higher column curve in the Canadian steel design standard [20]. The effective relief of cold-forming-induced residual stress due to hot-dip galvanizing has also been substantiated by research on galvanized regular- and high-strength RHS members under axial compressive and flexural loads [6,8-9]. Similar levels of residual stress reductions in CHS members after galvanizing were observed by [2].

In all, it can be concluded that similar to cold forming and welding, post-fabrication hot-dip galvanizing can also effectively change residual stress magnitudes and distributions in HSS. However, research on its effect on stress concentration and fatigue behaviour of connections in welded tubular steel truss/girder is limited. This paper focuses on welded RHS-to-RHS connections.

For fatigue behaviour of steel connections under cyclic loading, the effect of residual stress can be beneficial or detrimental, depending on its sign and magnitude. Tensile residual stress can often be detrimental since it accelerates the initiation and propagation of fatigue cracking. On the other hand, compressive residual stress can in general improve connection fatigue resistance [21]. Hence, methods such as hammer peening and shot

peening are available to reduce tensile residual stresses in steel connections by introducing compressive residual stresses.

For welded HSS connections, the fatigue resistances are commonly correlated to localized hot spot stress ranges at various locations around the joint. The fatigue resistances (i.e., permissible number of load cycles) can be determined based on calculated hot spot stress ranges and fatigue strength curves (S-N curves). For fatigue design of onshore tubular steel structures, the approach in CIDECT Design Guide 8 [21] is widely used internationally. As mentioned in this guide, this approach acknowledges the sign and magnitude of both residual and applied stresses by incorporating in connection fatigue resistance calculation the concept of stress range rather than the stress ratio. However, this approach was developed based on research on ungalvanized connections. In other words, the inevitable change of residual stresses around the perimeter of welded joint due to galvanizing, especially at the hot spot locations, is not considered in this approach.

In theory, connection fatigue resistance is affected by the sum of residual and applied stresses. In other words, the relative effect of residual stress varies at different external load levels. Hence, this research not only measures the residual stress changes due to cold forming, welding and galvanizing in the RHS connection specimens but also quantifies their effects on stress concentrations at various critical locations and different load levels based on the existing approach in CIDECT Design Guide 8 [21].

Chapter 3. Experimental program

3.1. Connection specimens

The experimental program includes four RHS-to-RHS X-connection specimens (Table 2). The RHS materials used to fabricate the four connection specimens were produced to Grade 350W Class C according to CSA G40.20/G40.21 [12]. The material has a nominal yield strength of 350 MPa and a nominal tensile strength of 450 MPa. All connections were fabricated with single-pass fillet welds of nominal leg size of 5 mm using matching E49XX electrodes (with an ultimate tensile strength of 490 MPa) [20] and a flux-cored arc welding-gas shielded process [22]. The welding process specifications used for the joints were: voltage = 25 V, amperage = 260 A, and travel speed = 230 mm/min. A typical connection with the symbol definitions is shown in Fig. 2. All four connection specimens have a branch-to-chord angle (θ) of 90°. As shown in Table 2, each specimen ID includes two components. The first component distinguishes the specimen by its fabrication process, where X = ungalvanized X-connection; and GX = galvanized X-connection. The second component is the branch-to-chord width ratio. The two galvanized specimens were dipped into and withdrawn from the same molten zinc bath at the same time. Hence, there is no variation in the temperature of the molten zinc bath. The hot-dipping process has a duration of approximately five minutes which is the current industry practice [1]. The selection of the specimens enables direct comparisons of the effects of galvanizing, as well as cold forming and welding, on the residual stresses in RHS connections with different branch-to-chord width ratios.

Based on St. Venant's principle and the suggestions by [23-27], all connections have sufficient branch and chord member lengths to ensure that the isolated connection specimens behave the same as those in a full truss/girder. On each side of any connection specimen, the branch length equals $3b_1$. For chord length, e in Fig. 2 equals $3b_0$. Therefore, $\alpha = 2l_0/b_0 = 2(6b_0+b_1)/b_0 > 4$, which meets the minimum chord length requirement in the CIDECT Design Guide 8 [21].

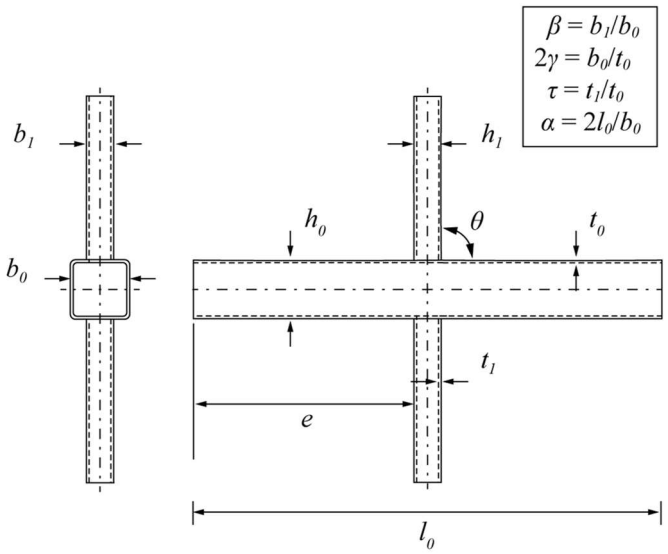

Fig. 2. Typical connection specimen and symbol definitions

Table 2. Nominal dimensions of connection specimens

Specimen ID	Chord (b_0×h_0×t_0) (mm)	Branch (b_1×h_1×t_1) (mm)	$\beta = b_1/b_0$	$2\gamma = b_0/t_0$	$\tau = t_1/t_0$
X-0.5	178×178×12.7	89×89×9.53	0.5	14	0.750
GX-0.5	178×178×12.7	89×89×9.53			
X-0.7	178×178×12.7	127×127×9.53	0.713	14	0.750
GX-0.7	178×178×12.7	127×127×9.53			

3.2. Material properties

This research measures the residual stresses on the chord surfaces of the four connection specimens. The rationale for selection of the 48 measurement locations is elaborated in Section 3.4. The material properties of the chord material before galvanizing (RHS 178×178×12.7 in Table 2) are determined via tensile tests on coupons cut from the additional length of the same parent RHS. Two tensile coupons from a flat face away from the weld seam were machined and tested according to the recommended procedures in ASTM A370 [28]. The material yield strength was determined using the 0.2% strain offset approach. The average value of the key material characteristics are as follows: yield strength (f_y) = 403 MPa; ultimate strength (f_u) = 495 MPa; Young's modulus (E) = 194.8 GPa; and rupture strain (ε_{rup}) = 34.9% (Appendix I). The rupture strain was determined by re-joining the fractured tensile coupon and measuring: the change in gauge length / initial gauge length.

3.3. Setup for measurements

The hole-drilling method measures the localized residual stresses on the surface of a component at the location of interest. Therefore, it is particularly suitable for this research as HSS connection fatigue behaviour is affected by localized residual stresses near the welded joint [21]. In this research, a specialized microscope, a standard high-speed air turbine hole-drilling device and standard strain gauge rosettes as recommended by ASTM E837 [29] were used to measure the residual stresses (Fig. 3). The hole-drilling process causes negligible damage to the steel component and hence is a semi-destructive method. The determination of residual stress is by releasing the localized stresses (via hole-drilling) and measuring the changes of strains in the nearby material. The measured changes of strains can then be used to calculate the in-situ residual stresses (i.e., before hole-drilling) using the procedures specified in ASTM E837 [29].

For each of the four connection specimens, in order to properly mount the hole-drilling device on the chord surface, a part of a branch is removed using a cold saw prior to the residual stress measurement. The cutting location was 40 mm away from the welded joint (Fig. 4). Coolant was used and the temperature of the cutting face was monitored during the entire course of cutting. In this case, the residual stresses on the measuring side due to cold forming and welding are fully retained, while the thermal effect from cutting is negligible. In other words, the residual stresses on the measuring side before and after cutting can be considered the same.

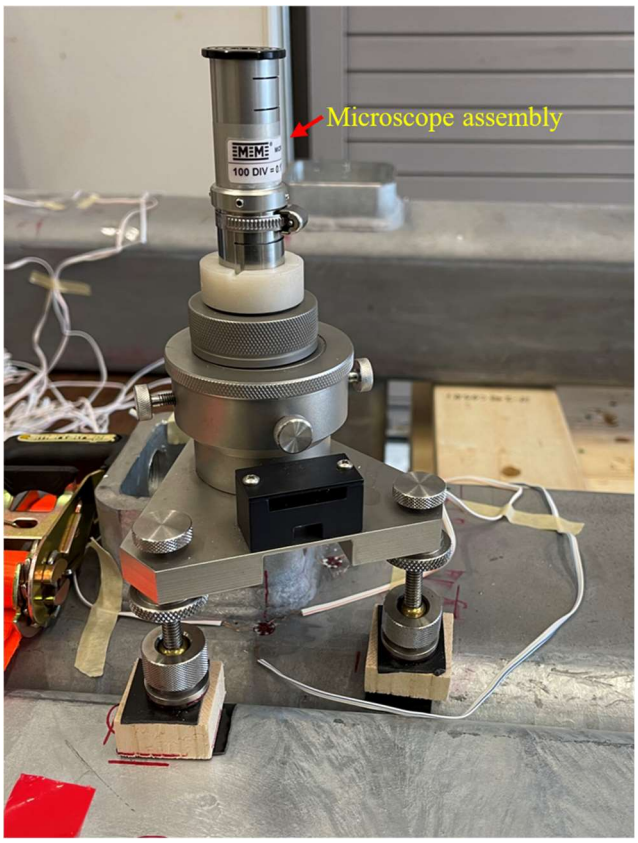

(a) Microscope assembly

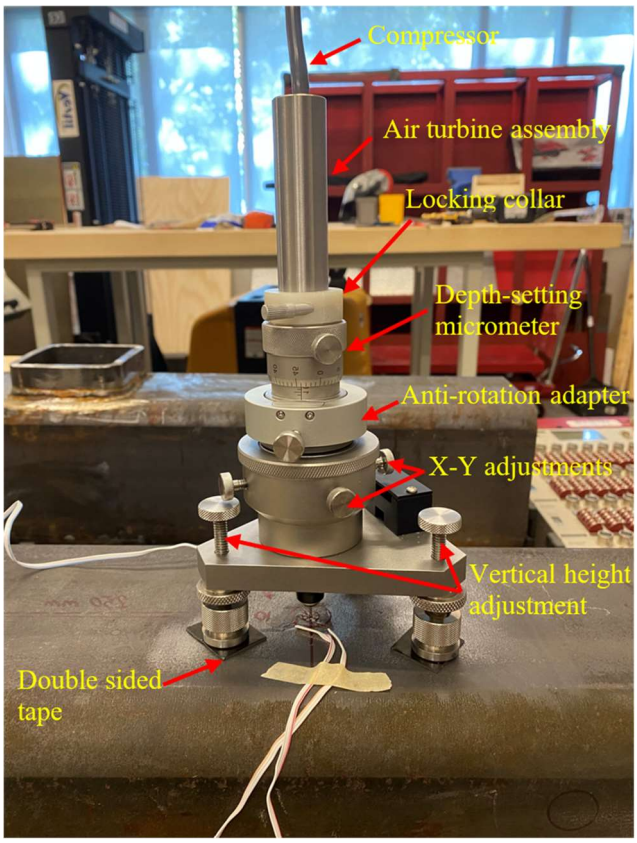

(b) High-speed air turbine assembly

Fig. 3. Equipment and setup recommended by ASTM E837 [29] for aliment and residual stress measurement

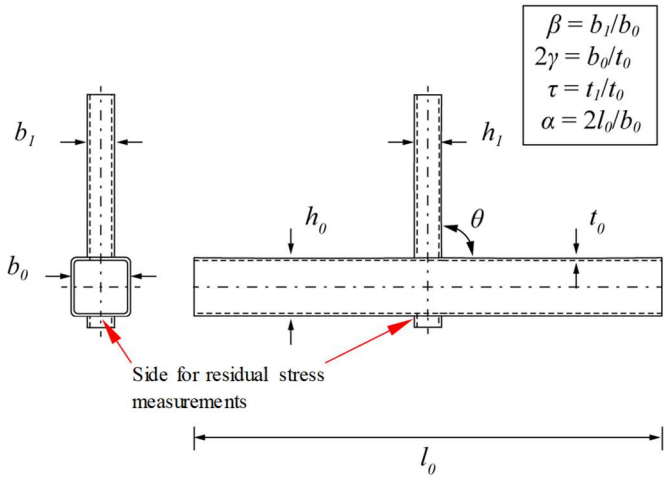

Fig. 4. Typical connection specimen after branch cutting

Prior to the installation of each strain gauge rosette, a pair of crossed reference lines were marked on the chord surface at the intended locations. The specialized microscope included in the hole-drilling device (Fig. 3(a)) was used to ensure accurate alignment of the strain gauge rosettes. Prior to the installation of strain gauge rosettes on the galvanized connection specimens, the zinc layer on the chord surface was carefully ground off using sandpaper. Detailed steps for strain measurements and stress calculations can be found in [13,15,16]. Therefore, no attempt is made in this paper to repeat the information. The high-speed air turbine assembly for hole drilling is shown in Fig. 3(b). Standard Type A strain gauge rosettes fully conforming to ASTM E837 [29] were installed. Therefore, the residual stress calculation rules in ASTM E837 [29] can be used. The strain gauge rosettes were carefully installed adjacent to weld toe to measure the localized residual stresses at the locations of interest.

3.4. Locations of strain gauge rosettes

For fatigue design of tubular steel connections, CIDECT Design Guide 8 [8] applies the hot spot stress approach. For RHS T- and X-connections, the hot spot stresses at the five critical locations (A to E in Fig. 5) are calculated by multiplying the nominal stress with the stress concentration factors (SCFs). The CIDECT Design Guide 8 formulae for the calculation of the SCFs at the hot spots under branch axial force are shown as Eqs. (1)-(4). The connection fatigue resistance can be estimated by pairing the calculated hot spot stresses with the fatigue strength (S-N) curves.

- Branch SCFs at hot spots A and E:

$$SCF_A = SCF_E = (0.013 + 0.693\beta - 0.278\beta^2)(2\gamma)^{(0.790+1.898\beta-2.109\beta^2)} \quad (1)$$

- Chord SCFs at hot spots B, C, and D:

$$SCF_B = (0.143 - 0.204\beta + 0.064\beta^2)(2\gamma)^{(1.377+1.715\beta-1.103\beta^2)}\tau^{0.75} \quad (2)$$

$$SCF_C = (0.077 - 0.129\beta + 0.061\beta^2 - 0.0006\gamma)(2\gamma)^{(1.565+1.874\beta-1.028\beta^2)}\tau^{0.75} \quad (3)$$

$$SCF_D = (0.208 - 0.387\beta + 0.209\beta^2)(2\gamma)^{(0.925+2.389\beta-1.881\beta^2)}\tau^{0.75} \quad (4)$$

Eqs. (1)-(4) are valid for: $0.35 \leq \beta \leq 1.0$, $12.5 \leq 2\gamma \leq 25$, $0.25 \leq \tau \leq 1.0$. For all hot spots, CIDECT Design Guide 8 [21] recommends a minimum SCF of 2.0. For connections with fillet welds, SCF_A and SCF_E are multiplied by 1.4.

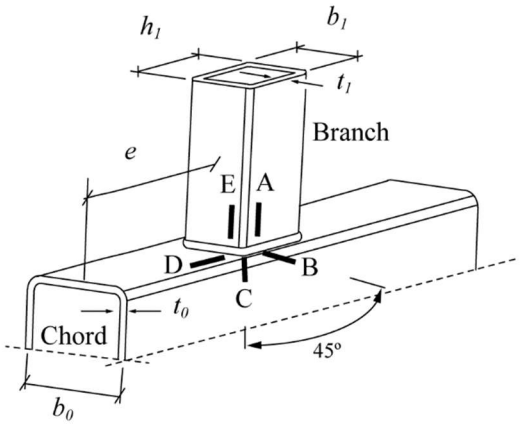

Fig. 5. Hot spot locations recommended by CIDECT Design Guide 8 [21]

In this study, the residual stresses were measured using the hole-drilling method and a total of 48 strain gauge rosettes (with 144 strain gauge elements) at 48 locations of interest on the four connection specimens. The overall approach is similar to previous research [13] on residual stresses in high-strength steel built-up connection with and without heat treatment where a comprehensive measurement was taken on two connection specimens at the critical locations around the welded joints. In the previous research [13], the measurements were performed on hot spots B, C and D in Fig. 5, since according to CIDECT Design Guide 8 [21], for RHS connections the highest SCFs often occur on the chord surface, which govern the connection fatigue resistance. Therefore, same as [13], in this study, the residual stresses are measured on the chord surface. The strain gauge rosette locations for connection specimens X-0.5 and GX-0.5 are shown in Fig. 6. The circular rosettes have a gauge circle diameter of 5.13 mm. Each rosette has three linear strain gauge elements. As shown in Fig. 6, the orientations of all rosettes were carefully selected to have one of the three linear strain gauge elements perpendicular to the weld and very close to the weld toe. The distances between the linear strain gauge elements perpendicular to weld and the weld toe are practically zero. This objective is to accurately determine the residual stress perpendicular to the weld at the weld toe location, which is relevant to the CIDECT Design Gudie 8

provisions [8]. For connection specimens X-0.7 and GX-0.7, the strain gauge rosettes are installed at similar locations. This section explains the rationale for the selection of rosette locations.

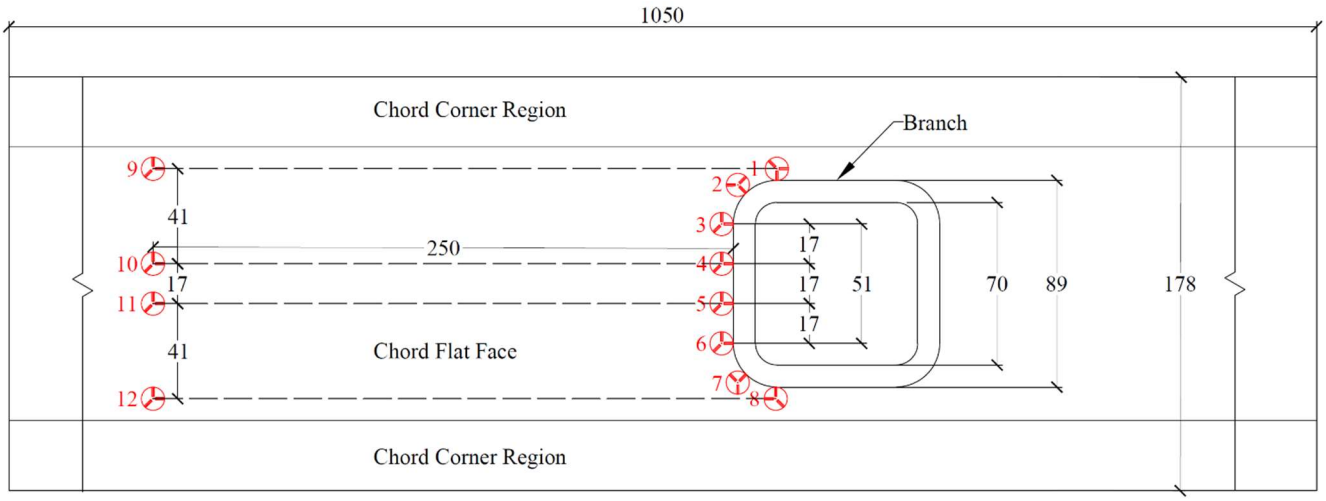

Fig. 6. Locations of strain gauge rosettes on X-0.5 and GX-0.5 (Unit: mm)

As shown in Fig. 6, strain gauge rosettes #1 to 8 are installed at the weld toe at the joint locations. Strain gauge rosettes #9 to 12 are installed at a location far away from the welded joint. In particular, rosette locations # 1 to 3 and #6 to 8 are consistent with the recommended hot spots B, C and D in Fig. 5. The primary sources of residual stresses of all measurement locations are listed in Table 3. The measurement locations are separated into four categories for the ungalvanized (X-0.5 and X-0.7) and galvanized (GX-0.5 and GX-0.7) connection specimens. As shown by the rationale in Table 3, the selected measurement locations (#1 to 12) allow for direct comparisons for quantification of residual stress changes due to cold forming, welding and galvanizing. For example, by comparing Categories I to III, the residual stress changes due to welding at the branch corner region of the welded joint can be determined. The measured residual stresses from the ungalvanized connections (X-0.5 and X-0.7) are compared to their galvanized counterparts (XG-0.5 and XG-0.7) in Section 4 to show the effects of galvanizing on residual stresses in connections with different branch-to-chord width ratios.

Table 3. Primary sources of residual stresses in connection specimens

Connection	Category	Location in Fig. 6	Primary sources of residual stresses
X-0.5 and X-0.7	I	# 1, 2, 3, 6, 7 and 8	Cold forming at chord corner region, and welding
	II	# 4 and 5	Cold forming at chord flat face, and welding
	III	# 9 and 12	Cold forming at chord corner region
	IV	# 10 and 11	Cold forming at chord flat face
XG-0.5 and XG-0.7	I	# 1, 2, 3, 6, 7 and 8	Cold forming at chord corner region, welding, and galvanizing
	II	# 4 and 5	Cold forming at chord flat face, welding, and galvanizing
	III	# 9 and 12	Cold forming at chord corner region, and galvanizing
	IV	# 10 and 11	Cold forming at chord flat face, and galvanizing

For comparison purpose, using the ASTM E837 rules [29], the residual stresses in the chord longitudinal and transverse directions ($\sigma_{rs,long}$ and $\sigma_{rs,tran}$ respectively) are determined at all measurement locations. The maximum principal residual stresses ($\sigma_{rs,p}$) are also determined for all measurement locations. $\sigma_{rs,p}$ is referred to as the principal residual stress hereinafter. It should be noted that the design recommendations in Eurocode 3 Part 1-9 [30] defines the hot spot stresses as "the maximum principal stress in the parent material adjacent to the weld toe, taking into account stress concentration effects due to the overall geometry of a particular constructional detail". Hence, the principal residual stresses are discussed in Section 5. On the other hand, CIDECT Design Guide 8 [21] defines the hot spot stresses as those perpendicular to the weld toe. Hence, in Section 6 the residual stresses perpendicular to the weld toe are determined and paired with the CIDECT SCF formulae to quantify the effects of galvanizing-induced residual stress changes on stress concentrations at the hot spots at different realistic fatigue load levels.

3.5. Residual stresses calculation

In order to calculate the residual stresses in different directions, the ASTM E837 uniform stress calculation method [29] is used with the specific dimensions of this particular program. The dimensions of the selected type

A strain gauge rosettes are listed in Appendix II along with the diameter of the drilled hole (D_0). The calibration constants $\bar{a}$ and $\bar{b}$ of each depth are determined by D_0 and calculated by linear interpolation (Appendix II). With the recorded relieved strain ε_1 (x-direction of strain gauge rosettes), ε_2 (45° direction of strain gauge rosettes) and ε_3 (y-direction of strain gauge rosettes), the uniform isotropic (equi-biaxial) strain (p), uniform 45° shear strain (q) and x-y shear strain (t) can be calculated by the following equation:

$$p = (\varepsilon_3 + \varepsilon_1)/2 \tag{5}$$

$$q = (\varepsilon_3 - \varepsilon_1)/2 \tag{6}$$

$$t = (\varepsilon_3 + \varepsilon_1 - 2\varepsilon_2)/2 \tag{7}$$

While the uniform isotropic (equi-biaxial) stress (P), uniform 45° shear stress (Q) and x-y shear stress (T) can be written as:

$$P = -\frac{E}{1+\nu}\frac{\sum(\bar{a}p)}{\sum(\bar{a}^2)} \tag{8}$$

$$Q = -E\frac{\sum(\bar{b}q)}{\sum(\bar{b}^2)} \tag{9}$$

$$T = -E\frac{\sum(\bar{b}t)}{\sum(\bar{b}^2)} \tag{10}$$

The uniform normal stresses in x (σ_x) and y (σ_y) directions, the uniform shear xy-stress, the maximum (σ_{max}) and minimum (σ_{min}) principal stresses and the maximum principal stress direction (β) can be calculated in the following equations:

$$\sigma_x = P - Q \tag{11}$$

$$\sigma_y = P + Q \tag{12}$$

$$\tau_{xy} = T \tag{13}$$

$$\sigma_{max}, \sigma_{min} = P \pm \sqrt{Q^2 + T^2} \tag{14}$$

$$\beta = \frac{1}{2} arctan\left(\frac{-T}{-Q}\right) \tag{15}$$

For locations #2 and 7, the chord longitudinal and transverse directions have a 45° difference from the direction perpendicular to the weld seam. The rest unknown values for these locations were calculated using the constants σ_{max} and σ_{min} with the following equations:

$$\beta_{45} = \beta - 45° \tag{16}$$

$$P_{45} = \frac{1}{2}(\sigma_{max} + \sigma_{min}) \tag{17}$$

$$Q_{45} = \frac{\sigma_{max} - \sigma_{min}}{2\sqrt{1+\tan(2\beta_{45})}} \tag{18}$$

$$T_{45} = Q \cdot \tan(2\beta_{45}) \tag{19}$$

$$\sigma_{x,45} = P_{45} - Q_{45} \tag{20}$$

$$\sigma_{y,45} = P_{45} + Q_{45} \tag{21}$$

$$\tau_{xy,45} = T_{45} \tag{22}$$

Chapter 4. Experimental results and discussions

4.1. Summary

For the ungalvanized connections (X-0.5 and X-0.7) and the galvanized connections (GX-0.5 and GX-0.7), the measured residual stresses are shown in Figs. 7 to 10, respectively, and the calculation results are listed in Appendix III. In this section, using the rationale in Table 3, the residual stresses in Figs. 7 to 10 are compared to quantify the effects of cold forming, welding, and galvanizing. One of the main objectives is to examine whether the residual stress changes due to galvanizing are in the same order of those from cold forming and welding. Since the latter two are implicitly considered in the CIDECT Design Guide 8 [21] and Eurocode 3 Part 1-9 [30], the analysis in this section aims to determine: (1) whether it is conservative or unconservative to use the existing design recommendations for galvanized HSS connections; and (2) whether additional considerations should be given to galvanized HSS connections. The analysis in this section also provides the basis for further analysis in Section 6 which is based on the residual stresses perpendicular to the weld seam.

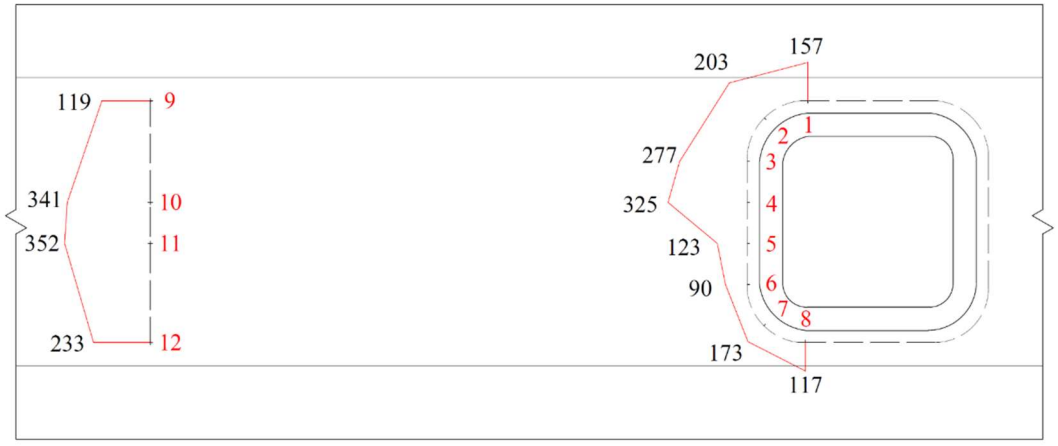

(a) Residual stresses in chord longitudinal direction ($\sigma_{rs,long}$)

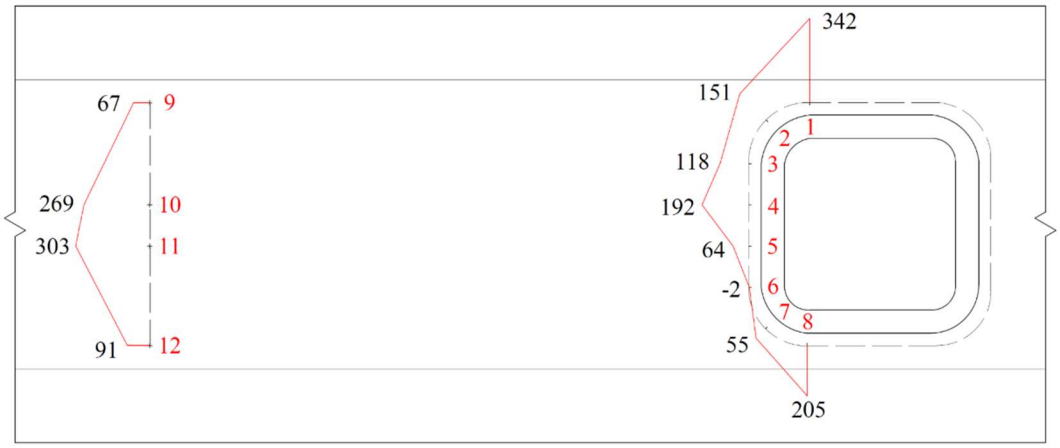

(b) Residual stresses in chord transverse direction ($\sigma_{rs,tran}$)

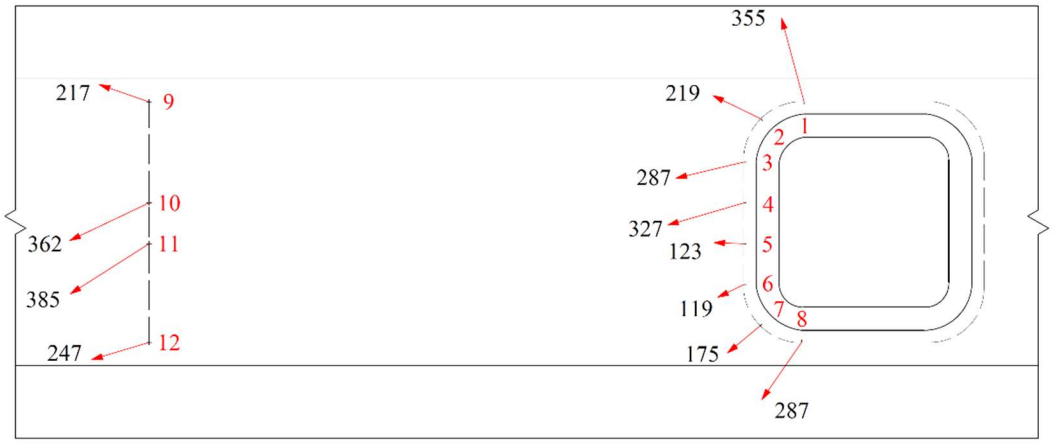

(c) Principal residual stresses and directions ($\sigma_{rs,p}$)

Fig. 7. Residual stresses in X-0.5 (Unit: MPa)

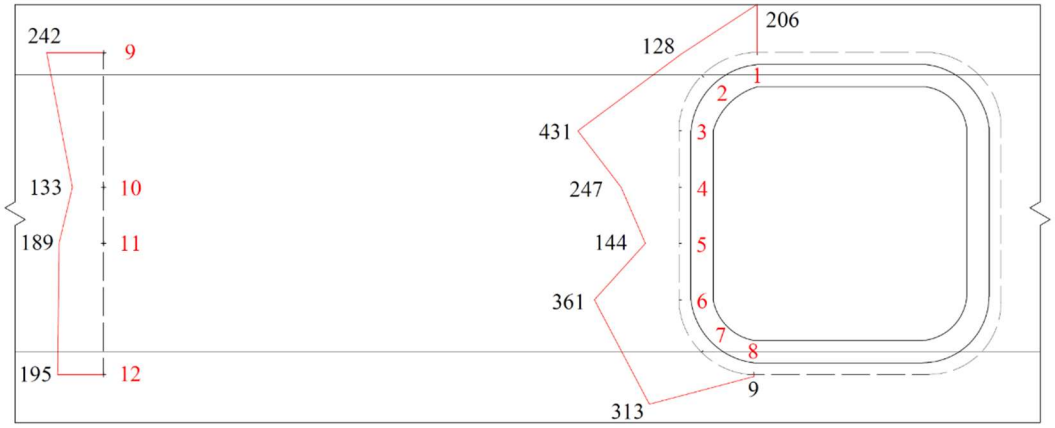

(a) Residual stresses in chord longitudinal direction ($\sigma_{rs,long}$)

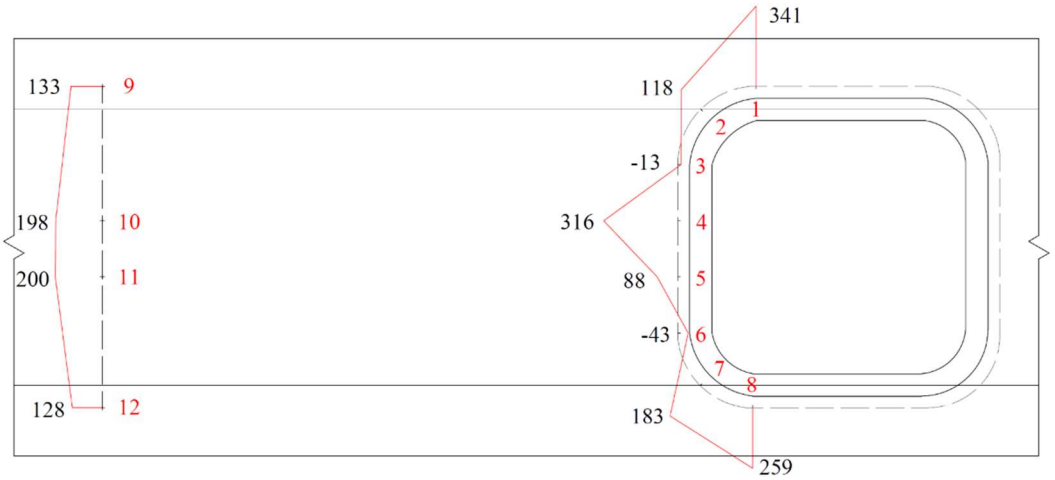

(b) Residual stresses in chord transverse direction ($\sigma_{rs,tran}$)

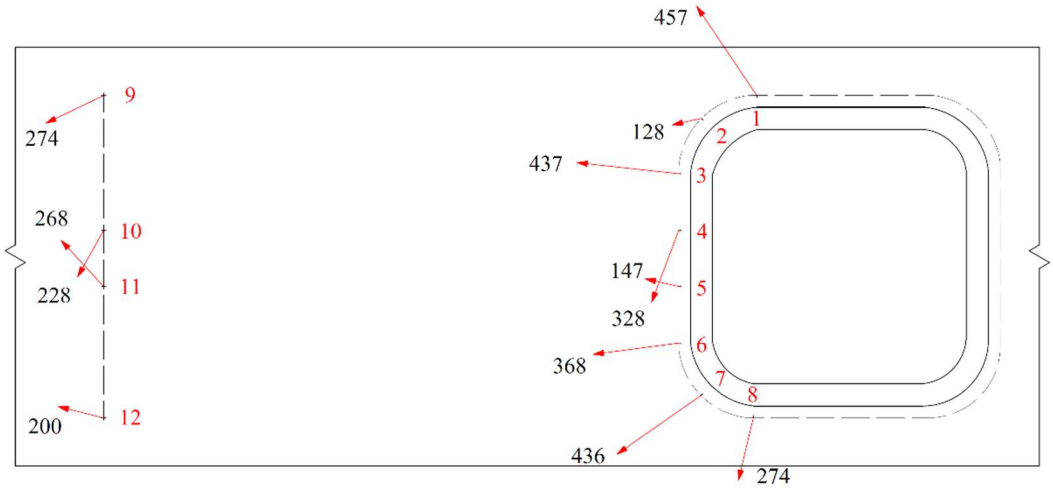

(c) Principal residual stresses and directions ($\sigma_{rs,p}$)

Fig. 8. Residual stresses in X-0.7 (Unit: MPa)

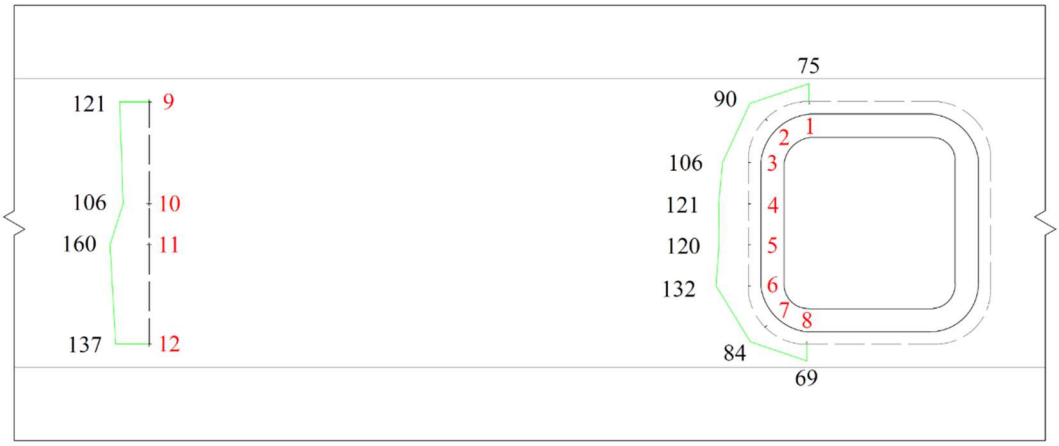

(a) Residual stresses in chord longitudinal direction ($\sigma_{rs,long}$)

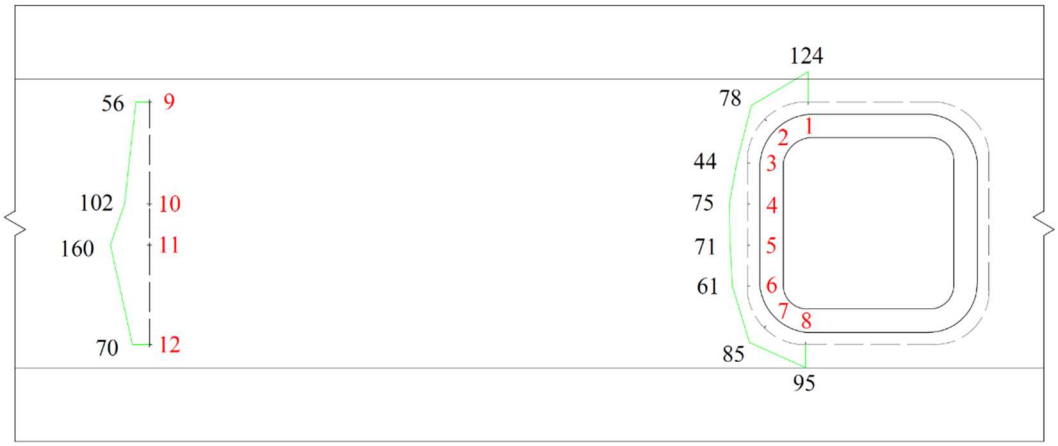

(b) Residual stresses in chord transverse direction ($\sigma_{rs,tran}$)

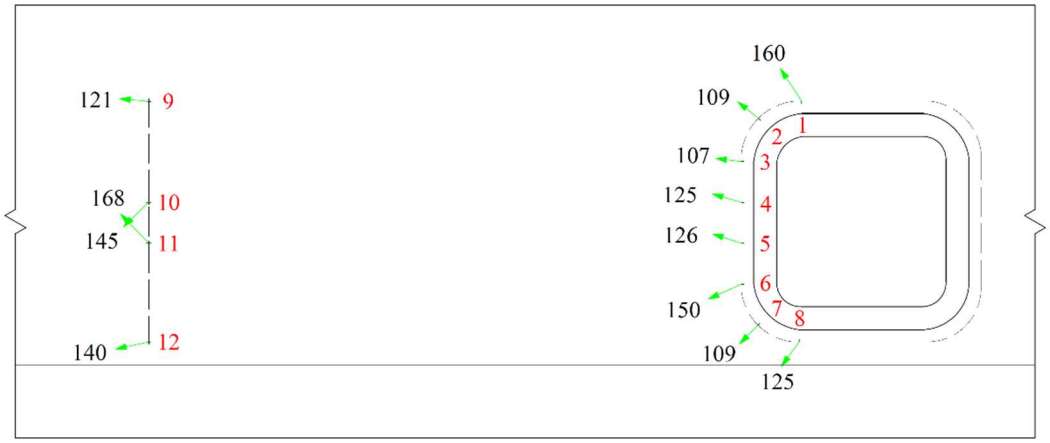

(c) Principal residual stresses and directions ($\sigma_{rs,p}$)

Fig. 9. Residual stresses in GX-0.5 (Unit: MPa)

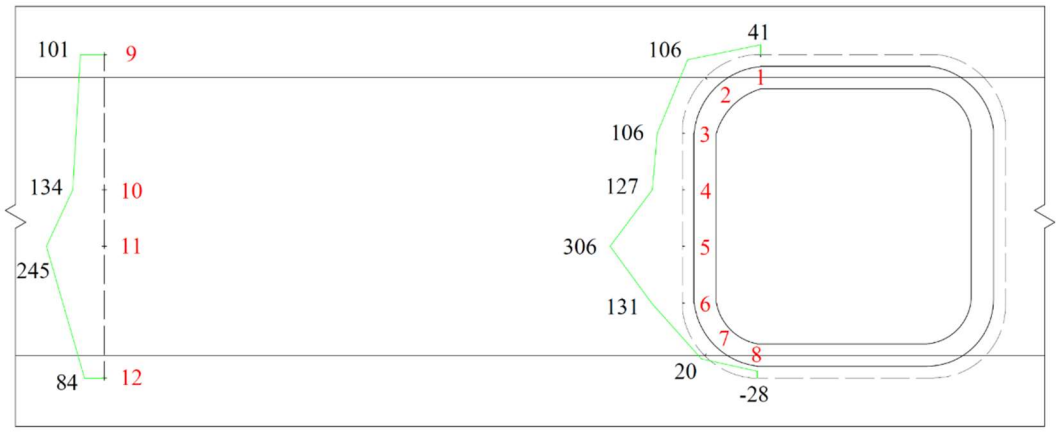

(a) Residual stresses in chord longitudinal direction ($\sigma_{rs,long}$)

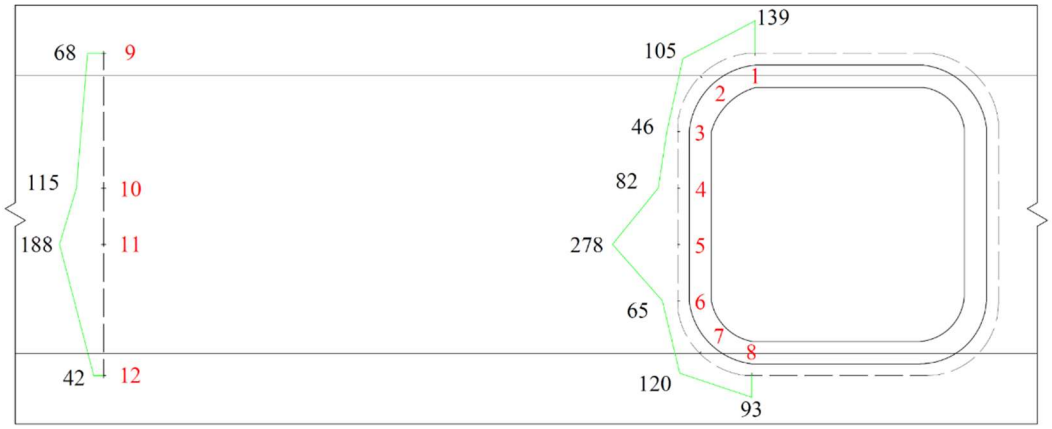

(b) Residual stresses in chord transverse direction ($\sigma_{rs,tran}$)

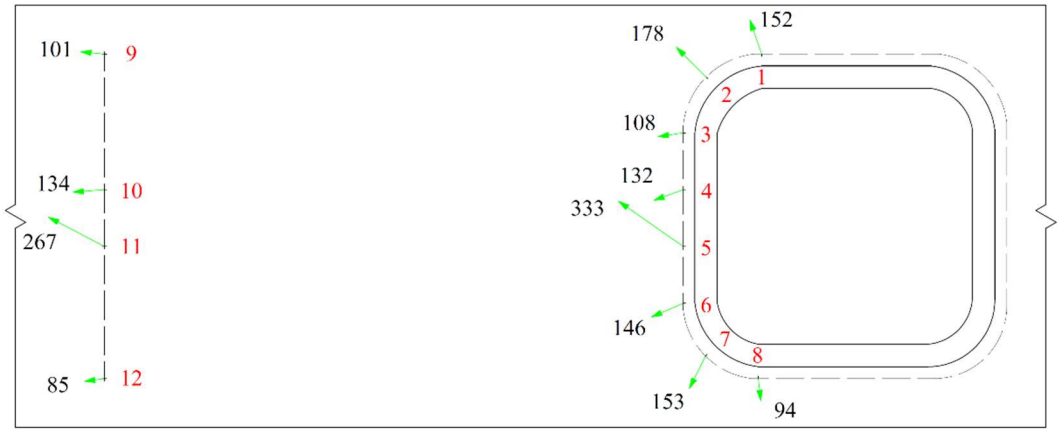

(c) Principal residual stresses and directions ($\sigma_{rs,p}$)

Fig. 10. Residual stresses in GX-0.7 (Unit: MPa)

4.2. Effects of cold forming

Cold working generates residual stresses in both the RHS longitudinal and transverse directions [7]. The measurement locations away from the welded joints (locations #9 to 12) in the ungalvanized connections (X-0.5 in Fig. 7 and X-0.7 in Fig. 8) are used to quantify the cold-working-induced residual stresses. In the figures, the positive values indicate tensile residual stresses while the negative values indicate compressive residual stresses. By comparing the longitudinal and transverse residual stresses at locations #9 to 12 in Figs. 7 and 8, the magnitudes in the two directions are in general similar, which is consistent with the findings in [31]. For design of RHS member under axial compressive and flexural loadings, the residual stresses in the member longitudinal directions are more relevant [10]. RHS wall elements with large compressive residual stresses in theory experience earlier reductions in stiffness and load-carrying capacity under axial compressive and flexural loadings [6-10]. As shown in Figs. 7 and 8, the measured residual stresses in the chord longitudinal locations away from the welded joints (i.e., locations #9 to 12) are tensile. This is consistent with the findings from [7]. For research on cold-formed RHS, the longitudinal residual stresses are typically resolved into membrane and bending components. The bending components are in general much greater than the membrane components and as a result govern the member behaviour under axial compressive and flexural loadings. In the theoretical model for the bending component, the residual stresses on the external and internal surfaces of the RHS wall have the same value but opposite senses. As shown in [7], when sectioning RHS into strips in the member longitudinal direction, all strips bend outwards. Hence, the in-situ longitudinal residual stresses, which keep all strips straight before sectioning, are tensile on the RHS external surface and compressive on the RHS internal surface. For the locations away from the welded joints (i.e., locations #9 to 12), although the hole drilling approach measures only the tensile residual stresses on the RHS external surfaces, it is expected that the compressive residual stresses on the internal surface are of similar magnitudes.

It should be noted that the chord members of all connection specimens are from the same RHS material (i.e., RHS 178×178×12.7 in Table 2). For locations #9 to 12 in Figs. 7 and 8, the longitudinal residual stresses away from the welded joint range from 119 to 352 MPa with an average value of 226 MPa, which is consistent with the values from various previous investigations listed in Table 1. Hence, credence can be given to the accuracy of the residual stress measurements in this study, which is important as the results herein forms the basis for

further evaluations on whether the residual stress changes due to galvanizing are in the same order of magnitude as those from cold forming and welding.

4.3. Effects of welding

Using the methodology in Table 3 and the results in Figs. 7 and 8, the effect of joint fabrication (mainly welding) on the residual stress magnitude and distribution around the welded joints can be estimated. For the connection with smaller branch-to-chord width ratio (X-0.5 in Fig. 7), the longitudinal residual stresses at the chord corner regions away from the welded joint (locations #9 and 12) range from 119 to 233 MPa with an average value of 176 MPa, which mainly come from cold working. After welding, the longitudinal residual stresses at the chord corner regions (locations #1 to 3 and 6 to 8) range from 90 to 277 MPa with an average value of 170 MPa. For the same connection specimen, the longitudinal residual stresses at the chord flat face away from the welded joint (locations #10 and 11) range from 341 to 352 MPa with an average value of 347 MPa. After welding, the longitudinal residual stresses at the same locations (locations #4 and 5) range from 123 to 325 MPa with an average value of 224 MPa. Hence, after joint fabrication, the residual stresses around the welded joint become less uniform. Similar observations can be made by comparing the residual stresses away from and at the welded joint of the connection with greater branch-to-chord width ratio (X-0.7 in Fig. 8).

It should be noted that the CIDECT Design Guide 8 [21] defines the hot spot stresses as those perpendicular to the weld toe. Hence, for locations #1 and 8 in Figs. 7 and 8, the transverse residual stresses are relevant for connection fatigue resistance as they correspond to hot spot B in Fig. 5. For locations #3 and 4 in Figs. 7 and 8, the longitudinal residual stresses are relevant for connection fatigue resistance as they correspond to hot spot D in Fig. 5. As shown in Figs. 7 and 8, comparing to the residual stresses away from the welded joint, the residual stresses at the hot spot locations perpendicular to the weld toe can sometimes change significantly (by a few hundred MPa). A comprehensive evaluation using only the residual stresses perpendicular to the weld toe is carried out for different hot spot locations and presented in Section 5 to quantify the effects of joint fabrication and galvanizing.

4.4. Effects of galvanizing

By comparing the residual stresses in the chord longitudinal and transverse directions ($\sigma_{rs,long}$ and $\sigma_{rs,tran}$ respectively) and the principal residual stresses ($\sigma_{rs,p}$) from the ungalvanized and galvanized connection specimens in Figs. 7 to 10, it can be seen that:

(1) In general, the residual stresses near the weld toes around the welded joints are tensile. After the application of post-fabrication hot-dip galvanizing, the residual stress distributions around the welded joint become more uniform and the maximum residual stresses become lower. Taking the hot spots recommended by CIDECT Design Guide 8 [21] as examples (i.e., measurement locations #1 to 3 and 6 to 8), the principal residual stresses for ungalvanized connection X-0.5 range from 119 to 355 MPa with an average value of 240 MPa. For its galvanized counterpart GX-0.5, the principal residual stresses range from 107 to 160 MPa with an average value of 127 MPa. Hence, an average principal residual stress reduction of 47% was observed at the hot spots recommended by CIDECT Design Guide 8 [21]. For the other set of connection specimens with greater branch-to-chord width ratios (X-0.7 and GX-0.7), an average principal residual stress reduction of 60% was observed. Hence, the levels of galvanizing-induced residual stress reductions at the hot spots are similar for the connection specimens with different branch-to-chord width ratios studied in this research.

(2) For the locations away from the welded joints (locations #9 to 12 in Figs. 7 and 9), as discussed in section 4.2, the longitudinal residual stresses range from 119 to 352 MPa with an average value of 226 MPa. After galvanizing, for the same locations in Figs. 8 and 10, the longitudinal residual stresses range from 84 to 245 MPa with an average value of 136 MPa. Hence, an average reduction of 39% was observed, which is consistent with the findings in [7].

(3) By comparing the above with the results in Sections 4.2 and 4.3, it can be concluded that the residual stress changes due to galvanizing are in the same order of those from cold forming and welding. Since the latter two are implicitly considered in the CIDECT Design Guide 8 [21] and Eurocode 3 Part 1.9 [30], further analysis based on the residual stresses perpendicular to the weld seam are performed and presented in Section 6, which is consistent with the hot spot stress approach from CIDECT Design Guide 8 [21].

Chapter 5. Stress concentrations at different fatigue load levels

5.1. Summary

The general steps in CIDECT Design Guide 8 [21] for calculation of welded HSS connection fatigue resistances are discussed in Section 3.4. The design guide uses the hot spot stress method where the hot spot stresses are defined as those perpendicular to the weld toe which can be determined by multiplying the nominal stress by the stress concentration factors. Same as CIDECT Design Guide 8 [21] and different from Eurocode 3 Part 1-9 [30], the design recommendations from the American Welding Society [32] and the American Petroleum Institute [33] also use hot spot stresses perpendicular to the weld toe rather than the principal stresses for the following reasons:

(1) Fatigue is a mechanism whereby cracks grow in a structure under fluctuating stresses, due to microstructural changes in the material. Cracks generally start at "discontinuities" which result in local stress concentrations. The geometric discontinuity at the weld toe in general results in localized significant increase in stresses perpendicular to the weld toe. However, its effect on localized stresses parallel to the weld toe is in theory minor. Hence, the difference between the localized stress perpendicular to the weld toe and the principal stress becomes smaller as the location becomes closer to the weld toe.

(2) When considering the stresses due to different loading and fabrication conditions, it is very difficult to combine the principal stresses in different directions from different cases.

Based on the above, in this section the stresses perpendicular to the weld toe, rather than the principal stresses, are used for further evaluation of the effects of post-fabrication hot-dip galvanizing. As shown by the example in Fig. 11, the residual stresses at locations #1 to 3 perpendicular to the weld toe are determined using the calculation rules from ASTM E837 [29]. These locations correspond to the CIDECT Design Guide 8 hot spots B to D shown in Fig. 5. Each residual stress in Fig. 11 is given an ID to show its location and direction. The first number indicates the location. The second number indicates the direction, where 0 = in the chord longitudinal direction; 45 = 45° away from the chord longitudinal direction; and 90 = in the chord transverse direction. As shown in the figure, $\sigma_{rs,1,90}$, $\sigma_{rs,2,45}$, and $\sigma_{rs,3,0}$ are directly relevant to the calculation using Eqs. (2) to

(4). The residual stresses at a location far away from the welded joint in the same directions ($\sigma_{rs,9,90}$, $\sigma_{rs,9,45}$, and $\sigma_{rs,9,0}$) are also determined (Appendix III). The same is carried out for the other side of each connection specimens for locations 6 to 8 and 12 in Fig. 11. The average values from the two sides of the connection are used for the following analysis:

(1) In Section 5.2, the differences between the residual stresses perpendicular to the weld seams in the ungalvanized and galvanized connection specimens are calculated. The significance of galvanizing-induced residual stress changes at different connection hot spots relative to various realistic fatigue load levels is evaluated.

(2) In Section 5.3, using the rationale in Table 3, the residual stresses perpendicular to the weld seams due to joint fabrications are determined. Such changes are combined with various realistic fatigue load levels to evaluate the significance of galvanizing-induced residual stress changes at different connection hot spots.

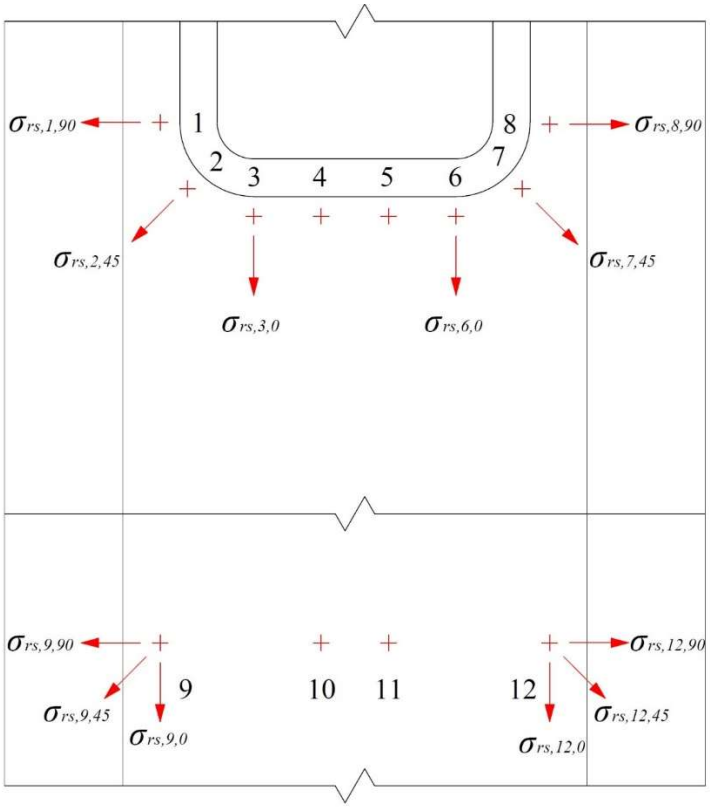

Fig. 11. Residual stresses perpendicular to weld toe

5.2. Effects of load level and galvanizing

In this section, the effect of joint fabrication is excluded. Using the CIDECT Design Guide 8 rules, the SCFs at the hot spots in the connection specimens are calculated using Eqs. (2) to (4) and the values are listed in Table 4. The approach used in the previous research on residual stress and stress concentration effect of high strength steel built-up box T-joints [32] is applied herein. Specifically, Eq. (23) is used to evaluate the significance of galvanizing-induced residual stress changes at the connection hot spots relative to realistic fatigue load levels.

Table 4. Stress concentration factors calculated using CIDEC Design Guide 8 rules [21]

SCF	Hot spot B	Hot spot C	Hot spot D
X-0.5	8.10	7.12	4.19
X-0.7	5.27	5.08	2.55

$$RSF_i = \frac{\left|\Delta\sigma_{rs.gal.i}\right|}{\left|\Delta\sigma_{rs.gal.i}\right| + SCF_i \cdot \sigma_n} \tag{23}$$

where

i = B, C and D in Fig. 5;

RSF_i = residual stress factor at hot spot i;

$\Delta\sigma_{rs,gal,i}$ = change of residual stress due to galvanizing at hot spot i;

SCF_i = stress concentration factor from Table 4 at hot spot i; and

σ_n = nominal stress under branch axial loading which can be calculated using the design recommendations in CIDECT Design Guide 8 [21].

It should be noted that based on the comparison of the experimental results in Figs. 7 to 10, $\Delta\sigma_{rs,gal,i}$ is always negative since post-fabrication galvanizing reduces the residual stresses. This is consistent with the findings in the recent experimental research [7] where for regular-strength RHS the bending residual stresses changed from 62% - 80% of the measured yield stresses to 33% - 50% after galvanizing, and for high-strength RHS the values

changed from 49% - 69% to 24% - 37% after galvanizing. Similar levels of residual stress reductions in CHS members after galvanizing were observed by another previous research [2].

Specifically, the residual stresses perpendicular to the weld seam (Fig. 11) at locations 1 to 3 and 6 to 8 are determined for all connection specimens for the evaluation herein. For each location, $\Delta\sigma_{rs,gal,i}$ is the difference between the residual stresses in the ungalvanized connection and their galvanized counterpart (X-0.5 versus GX-0.5 where β = 0.5, and X-0.7 versus GX-0.7 where β = 0.7). The average values are used as the residual stress changes at hot spots B, C and D. In Fig. 12, the galvanizing-induced residual stress changes are plotted against a nominal stress range from 0 to 50 MPa for the two β-values, considering the stress concentration values in Table 4 and that the RHS material nominal yield stress is 350 MPa.

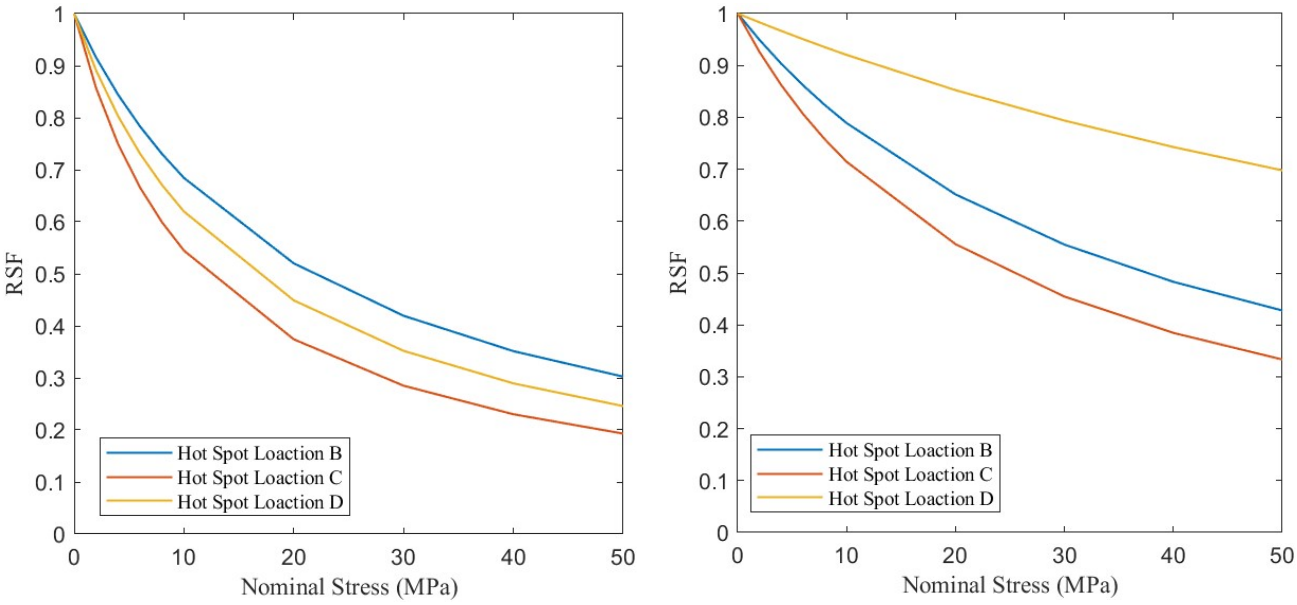

(a) β = 0.5 (b) β = 0.7

Fig. 12. Residual stress factor (RSF) distributions for hot spot locations in Fig. 5

It can be seen from Eq. 23 and Fig. 12 that:

(1) For the two different branch-to-chord width ratios, post-fabrication hot-dip galvanizing has a significant effect on the connection stress concentrations over the realistic branch nominal stress range.

(2) The higher the RSF-value, the larger the effect of galvanizing. The effects of galvanizing on stress concentrations at different hot spots are nonlinear over the branch nominal stress range. As the nominal stress (from branch axial loading) increases, the effect of galvanizing becomes smaller.

(3) The RSF-values in Figs. 12(a) and (b) for β = 0.5 and β = 0.7 are different which indicates that the effects of galvanizing on the two sets of connection specimens with different branch-to-chord width ratios are different. The effect of galvanizing is more significant for the connection with larger β-value. As discussed in Section 4.4, the levels of galvanizing-induced residual stress reductions at the hot spots are similar for the connection specimens with different β-ratios. In both cases (β = 0.5 and β = 0.7), the residual stresses at nearly all hot spots before galvanizing were reduced by approximately 50% after galvanizing. Hence, the effect of galvanizing is more significant for the connection with larger β-value because its SCFs are smaller (see Table 4), producing a smaller $SCF_i \cdot \sigma_n$-value in Eq. 5.

5.3. Effects of load level, joint fabrication and galvanizing

In this section, using the rationale in Table 3, the residual stresses perpendicular to the weld toes due to joint fabrications (mainly welding) are determined. Such changes are combined with various fatigue load levels to evaluate the significance of galvanizing-induced residual stress changes at different connection hot spots. For ungalvanized RHS T- and X-connections, CIDECT Design Guide 8 [21] recommends that the hot spot stresses can be calculated by multiplying the branch nominal stress with the SCFs. To initiate the analysis in this section, it is first assumed that the stress concentrations in galvanized RHS T- and X-connections can be evaluated using Eq. (24). The validity of this assumption is examined later in this section using the experimental results.

$$SCF_{gal,i} = SCF_i \cdot \psi_i \quad (24)$$

where

i = B, C and D in Fig. 5;

$SCF_{gal,i}$ = stress concentration factors for galvanized connection at hot spot i;

SCF_i = stress concentration factors for ungalvanized connection at hot spot i which can be calculated using the CIDECT Design Guide 8 formulae;

$$\psi_i = \frac{SCF_i \cdot \sigma_n + \Delta\sigma_{rs,fab,i} + \Delta\sigma_{rs.gal.i}}{SCF_i \cdot \sigma_n + \Delta\sigma_{rs.fab.i}} \quad (25)$$

where

ψ_i = residual stress correction factor considering the effect of galvanizing at hot spot i, where i = B, C and D;

σ_n = nominal stress under branch axial loading which can be calculated using the design recommendations in CIDECT Design Guide 8 [21];

$\Delta\sigma_{rs,fab,i}$ = change of residual stress due to joint fabrication at hot spot i;

$\Delta\sigma_{rs,gal,i}$ = change of residual stress due to galvanizing at hot spot i;

Specifically, the $\Delta\sigma_{rs,gal,i}$-values in Eq. (25) are determined using the approach from Section 5.2 for the connection specimens. The $\Delta\sigma_{rs,fab,i}$-values in Eq. (25) are the differences between the residual stresses at the welded joint location and the location far away from the welded joint in the same direction. For example, $\Delta\sigma_{rs,fab,B}$ is the average of the difference between $\sigma_{rs,1,90}$ and $\sigma_{rs,9,90}$ and the difference between $\sigma_{rs,8,90}$ and $\sigma_{rs,12,90}$. As mentioned in Section 5.2, $\Delta\sigma_{rs,gal,i}$ is always negative since post-fabrication galvanizing reduces the residual stresses, while $\Delta\sigma_{rs,fab,1}$ is in general positive. This is consistent with the findings in previous research listed in Table 1. The residual stress correction factors (ψ_i) are plotted against the nominal stresses in Figs. 13(a) and (b). It can be seen from the figures that:

(1) When considering the effect of joint fabrication-induced residual stress changes, for the two different branch-to-chord width ratios, post-fabrication hot-dip galvanizing also has a significant effect on the connection stress concentrations over the realistic branch nominal stress range.

(2) In Figs. 13(a) and (b), the smaller the ψ_i-value, the greater the effect of galvanizing. Similar to the third conclusion in Section 5.2, galvanizing has a greater effect on the connection with larger β-value because its SCFs are smaller (see Table 4) which produces smaller $SCF_i \cdot \sigma_n$-values in Eq. 7.

(3) When the applied nominal stress is relatively high (30 to 50 MPa), it may be reasonable to use the residual stress correction factor (ψ) and Eq. (24) to consider the effect of galvanizing on stress concentrations using the approach in CIDECT Design Guide 8 [21]. When the applied nominal stress is relatively low (10 to 30 MPa), the ψ-values in Fig. 13 are very low for all hot spots, and the application of Eq. (24) becomes problematic. This happens because the galvanizing-induced residual stress

reduction is greater than the hot spot stress ($SCF_i \cdot \sigma_n$). It is possible that, for the connection specimens studied, the galvanizing process has brought them to locations beyond the "cut-off limit" of the S-N curve (i.e., below the non-propagating stress limit where the fatigue life is indefinite). However, more experimental testing is needed to examine this speculation.

(4) Clear nonlinear trends for ψ can be observed for different hot spots in Fig. 13. Further experimental testing is needed to develop definitive design recommendations to consider the effect of galvanizing. However, it would be conservative to ignore the effect of galvanizing and use the existing CIDECT Design Guide 8 recommendations [21] to evaluate the stress concentrations in galvanized connections. It should be noted again that similar to heat-treated HSS (also at 450 °C) per ASTM A1085 Supplement S1 [11], or Class H HSS per CSA G40.20/G40.21 [12], the galvanizing temperature has little effect on the material strength and ductility (as a higher temperature is needed to produce metallurgical changes) [1].

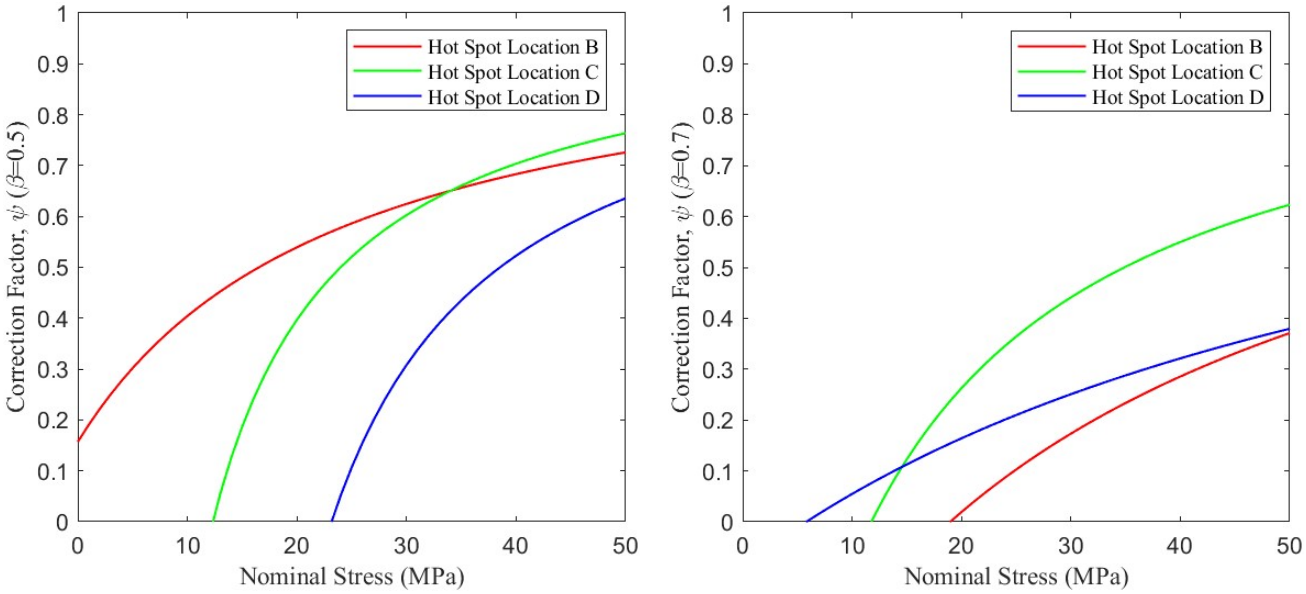

(a) $\beta = 0.5$ (b) $\beta = 0.7$

Fig. 13. Residual stress correction factor (ψ) distributions for hot spot locations in Fig. 5

Chapter 6. Testing of connection specimens under quasi-static branch axial loads

6.1. Test setup and instrumentation

6.1.1. Test specimens

After the residual stress measurements, the four RHS connection specimens were tested under quasi-static branch axial compressive forces to failure to examine whether post-fabrication hot-dip galvanizing has effects on the connection behaviours under static loading. The dimensions of the specimens are provided in Table 2.

6.1.2. Universal testing machine

The connection tests were conducted separately using a 1000-kN capacity Tinius Olsen machine and a 2000-kN capacity MTS universal testing machine. The X-0.5 and GX-0.5 connections were tested using the Tinius Olsen machine, while the X-0.7 and GX-0.7 connections were tested using MTS universal testing machine. The test setup is depicted in Fig. 14.

Fig. 14. Typical test setup

6.1.3. Support conditions

A pedestal on the machine frame base was used to support the short branch, while a steel plate was placed on top of the long branch to protect the testing machine. This support configuration enabled the load to be transmitted through the branches and the chord center. Even though one branch had been cut, the connection was still an X-connection joint based on the method of force transfer.

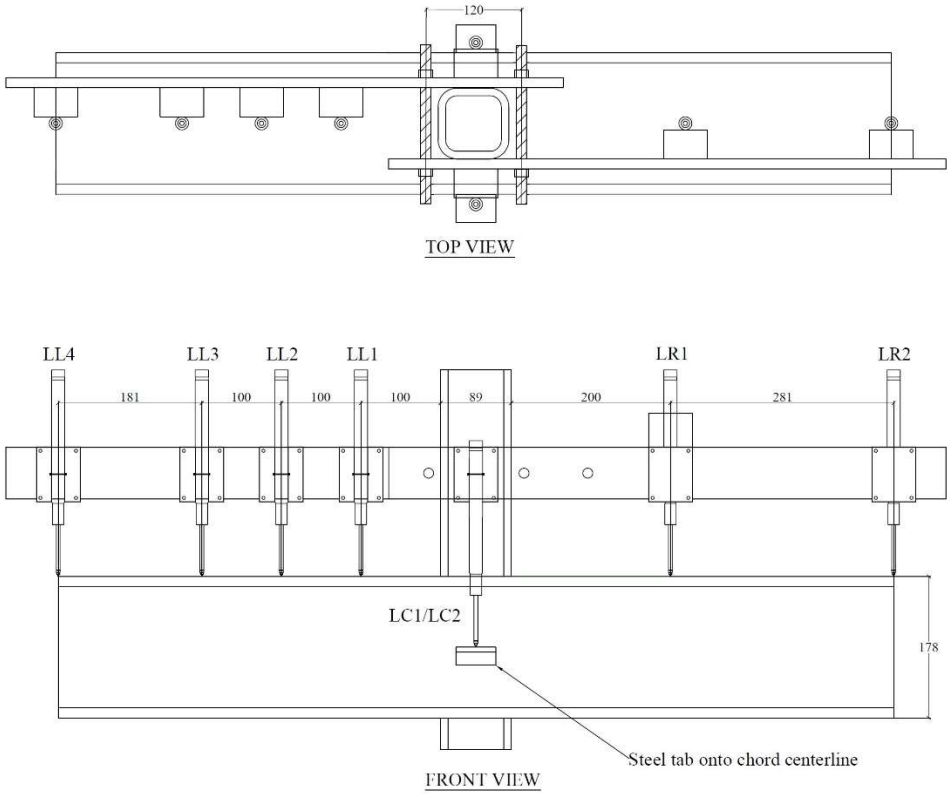

Fig. 15. Locations of Linear Variable Differential Transformers (LVDTs)

6.1.4. LVDTs

For each of the four connection specimens, a total of eight Linear Variable Differential Transformers (LVDTs) were used to record the deformation along the entire chord length. A typical setup and the LVDT locations are shown in Figs.14 and 15, respectively. Specifically, LL1, LL2, LL3, LL4, LR1, and LR2 are consistent with the readily adopted hollow section connection research convention [35] to measure displacements perpendicular to the chord top surface. Similar measurements from LL2 and LR1 as well as LL4 and LR2 were expected due to the symmetry of connection configuration and loading condition. Connection displacement (δ) is conventionally defined as the localized deformation of the connection where the branch and chord centrelines meet. It is typically measured from the connection work point to a reference point on the branch. In this research, as shown in Fig. 15, the connection displacement is measured by using two central LVDTs (LC1 and LC2) in conjunction with two steel plates welded onto the chord centerlines on the two chord sides. The average reading of the LC1 and LC2 was used to establish the connection load-displacement curve.

6.2. Failure modes

In accordance with the recommendations of the CIDECT Design Guide 3 [35], the connection capacity at the ultimate limit state was determined as the lower value of the maximum load and the load corresponding to the $3\%b_0$ (5.34mm) deformation limit. After this ultimate limit state was reached, the connection specimens were considered to have failed.

6.3. Test results

Displacement-controlled tests were performed on the four connection specimens at a rate of 0.2 mm per second to connection failure. The branch axial load-connection displacement curves (based on the average readings from LC1 and LC2) are presented in Fig. 16, $N_{1,u}$ represents the maximum branch axial load, while$N_{1,3\%}$ represents the branch axial load corresponding to the $3\%b_0$ deformation limit. Fig. 17 shows the typical failure modes with clear yield line patterns. The overall deformed shapes of the ungalvanized (X-0.5 and X-0.7) and the galvanized (GX-0.5 and GX-0.7) connection specimens are very similar. All four connection specimens were governed by the limit state of chord wall plastification. The chord top face deformation profiles for all connection specimens (based on all LVDT readings) at different load levels are shown in Fig. 18.

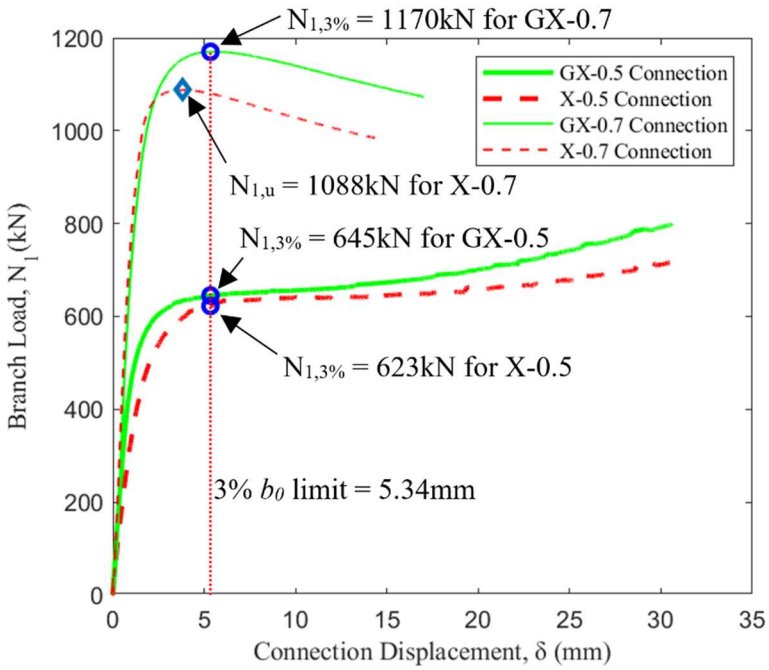

Fig. 16. Load-displacement curves

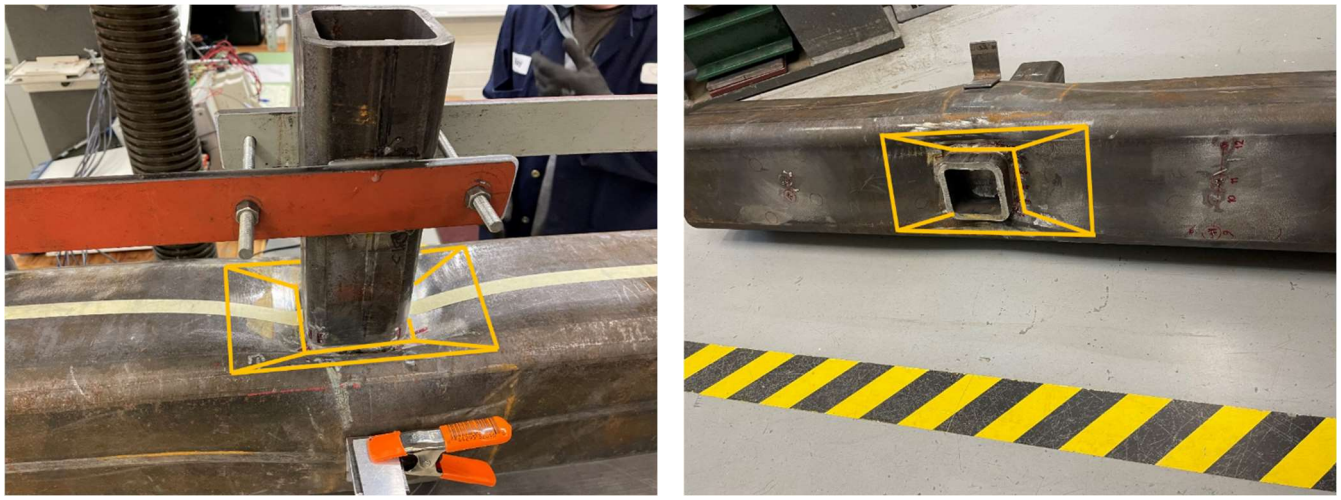

Fig. 17. Typical failure mode

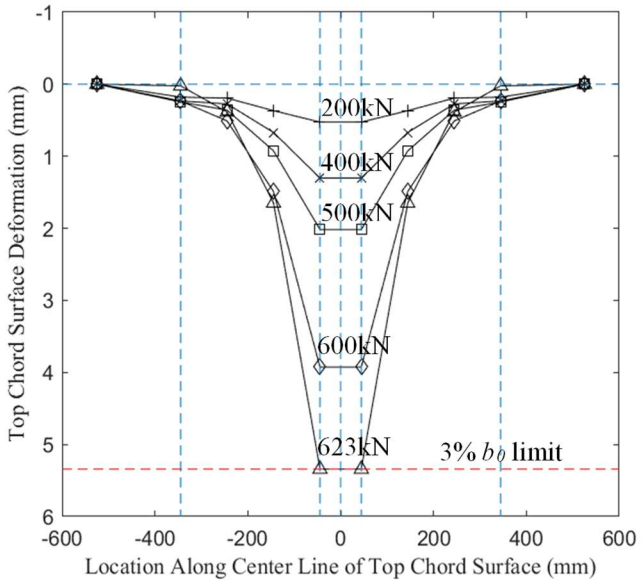

(a) X-0.5

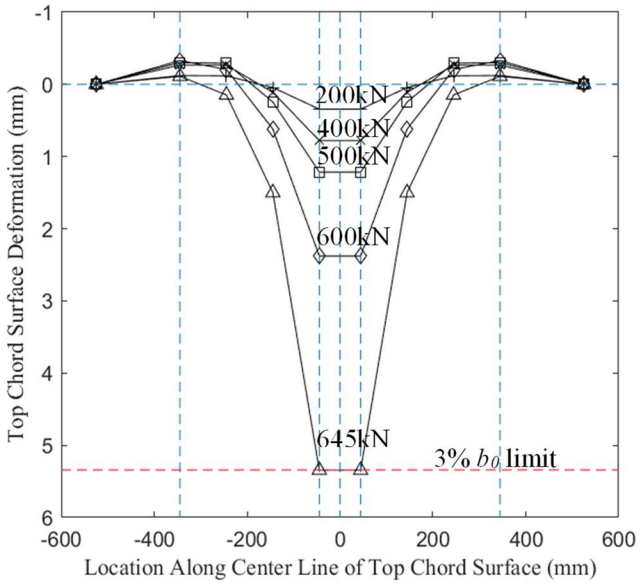

(b) GX-0.5

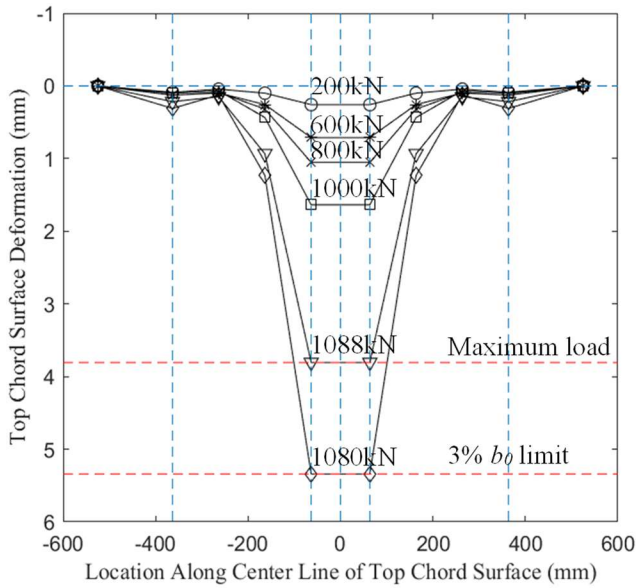

(c) X-0.7

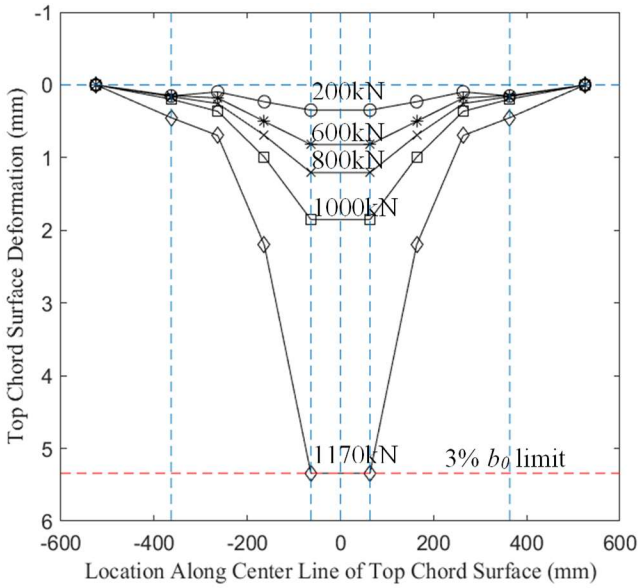

(d) GX-0.7

Fig. 18. Chord face deformation profiles

6.4. Discussions of connection test results

By comparing the test results of the ungalvanized and galvanized connection specimens with different branch-to-chord width ratios (β) in Figs. 16 to 18, it can be seen that:

(1) For the two connections with β = 0.7, the galvanized specimen (GX-0.7 where $N_{1,3\%}$ = 1170 kN) has a connection strength 8% greater than its ungalvanized counterpart (X-0.7 where $N_{1,u}$ = 1088 kN). For the ungalvanized specimen (X-0.7), the maximum branch axial load ($N_{1,u}$) occurred before the 3%b_0 deformation limit during testing and hence the former was considered as the connection capacity. On the other hand, for the galvanized specimen (GX-0.7), the load at the 3%b_0 deformation limit was determined as the connection capacity at the ultimate limit state. This suggests a minor ductility increase due to the post-fabrication hot-dip galvanizing.

(2) For the two connections with β = 0.5, the galvanized specimen (GX-0.5 where $N_{1,3\%}$ = 645 kN) has a connection strength slightly greater than its ungalvanized counterpart (X-0.5 where $N_{1,3\%}$ = 623 kN). However, as shown in Fig. 19, the load-displacement curve for the GX-0.5 deviated from the linear-elastic behaviour at a much later stage compared to its ungalvanized counterpart (X-0.5). This suggests a reduction of residual stress due to the post-fabrication hot-dip galvanizing which is consistent with the findings based on the residual stress measurements discussed in the earlier sections of the paper.

(3) By comparing the chord face deformation profiles of the connection specimens in Fig. 18, it can also be seen that at different load levels, the deformations of the chord top surface of galvanized connections are always less severe than their ungalvanized counterparts, indicating improvements of connection behaviours after galvanizing.

(4) Conservatively, galvanized RHS connections under predominantly static loading can be designed using the same design rules for ungalvanized RHS connections.

Chapter 7. Conclusions

This paper represents a first step towards understanding the effects of post-fabrication hot-dip galvanizing on residual stresses in welded tubular steel connections. In this study, the residual stresses and stress concentrations in galvanized rectangular hollow section (RHS) connections has been investigated comprehensively for the first time, using the hole-drilling approach and a total of 144 strain gauge elements at different locations of four connection specimens.

Based on the experimental results in this study, it was found that:

(1) Similar to the heat treatment (at 450 °C) per ASTM A1085 Supplement S1 [11] and the Class H finish per CSA G40.20/G40.21 [12], the commonly applied post-production hot-dip galvanizing process (at 450 °C) reduces the residual stresses in cold-formed RHS members and connections. It should be noted that previous research [1-10] showed that the galvanizing temperature has little effect on the steel material strength and ductility as a higher temperature is needed to produce metallurgical changes.

(2) For the connection specimens with different branch-to-chord width ratios studied in this research, the levels of galvanizing-induced residual stress reductions at the hot spots (for fatigue design) are similar.

(3) The galvanizing-induced residual stress changes are in the same order of those from cold forming and welding and hence will in theory affect the connection fatigue performance.

(4) As the branch nominal stress increases, the effect of galvanizing on stress concentration becomes smaller.

(5) For the connection specimens in this study, the effect of galvanizing on stress concentration is more significant for the connection specimens with larger β-values.

(6) Further research is needed to develop definitive design recommendations to be used in conjunction with the existing CIDECT Design Guide 8 recommendations [21] to evaluate stress concentrations in galvanized RHS connections.

(7) Based on the test results of the connection specimens under quasi-static branch axial forces, it was found that the galvanized connection specimens have slightly better performances. Hence, galvanized RHS connections under predominantly static loading can be designed using the same design rules for ungalvanized RHS connections.

Appendix I. Coupon test results

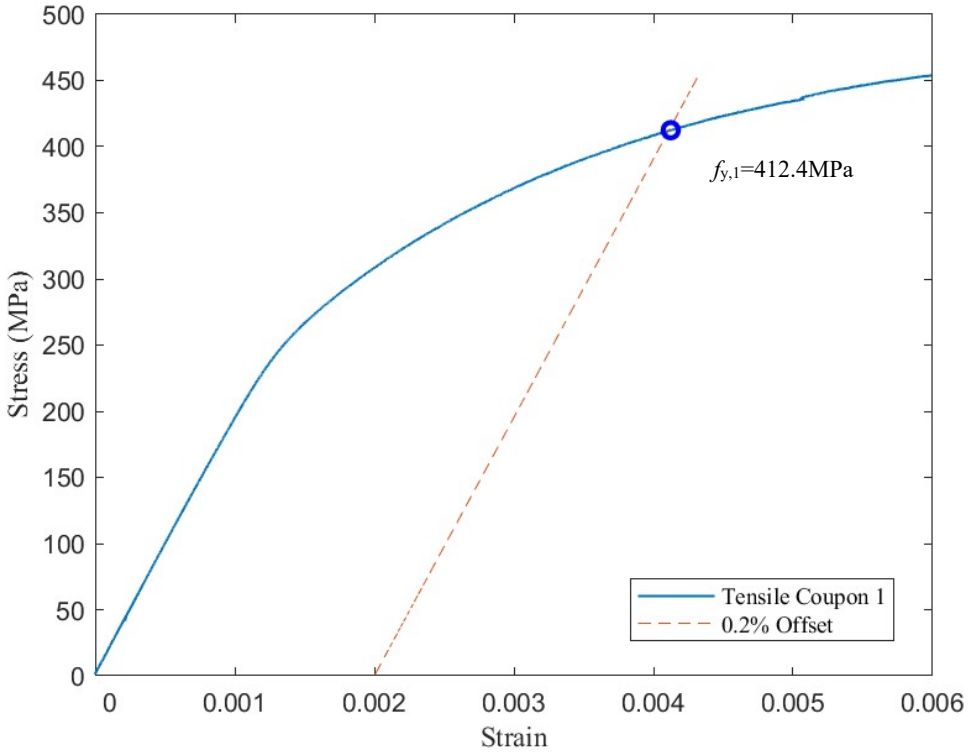

(a) Tensile coupon 1

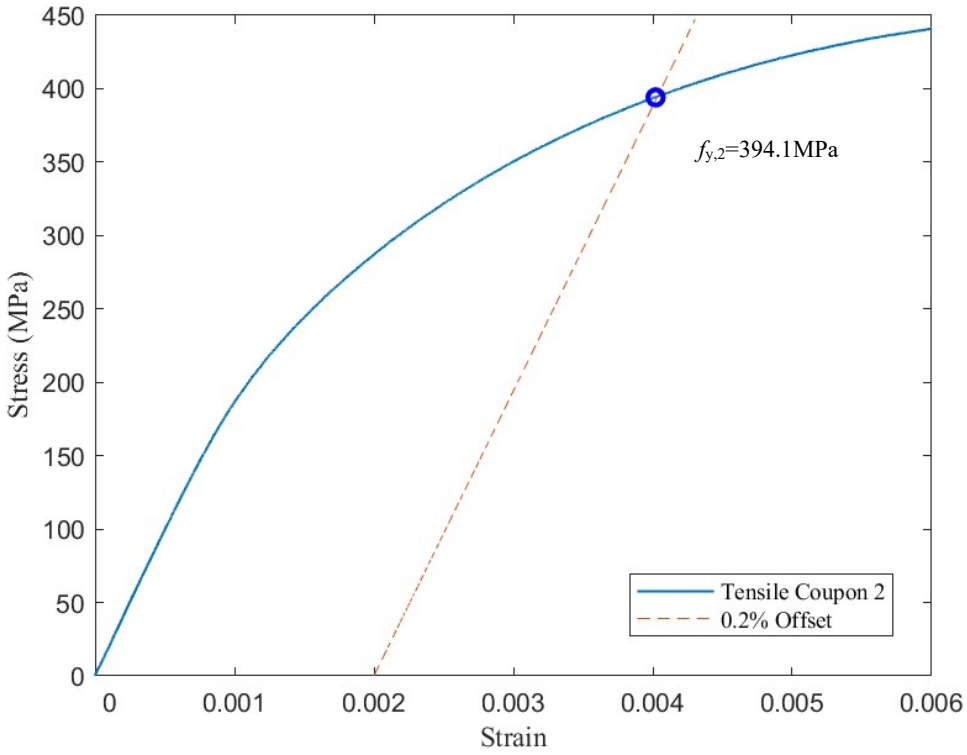

(b) Tensile coupon 2

Fig I.1. Tensile coupon stress-strain curves with the 0.2% offset yield strength

Table I.1. Tensile coupon test results

	Yield strength (MPa)	Ultimate strength (MPa)	Young's modulus (MPa)	Rupture strain (%)
Tensile Coupon 1	412.4	497.3	194116	34.79
Tensile Coupon 2	394.1	492.6	195384	34.91
Average Value	**403.3**	**494.9**	**194750**	**34.85**

Fig I.2. Tensile coupons after test

Appendix II. Type A strain gauge rosettes parameters

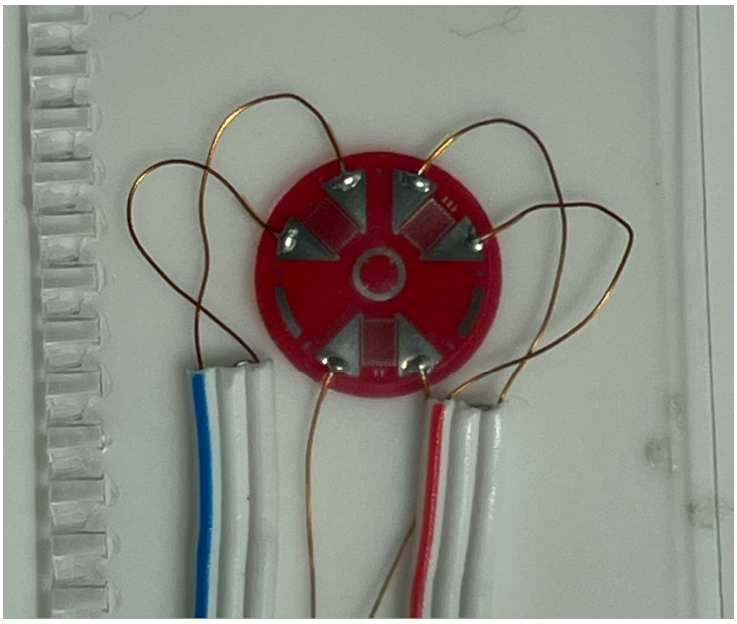

Fig II.1. Typical type A strain gauge rosette

Table II.1. Type A strain gauge rosette parameters

Rosette Type	D (mm)	D_0 (mm)	Practical Depth Steps (mm)
Type A 062RE	5.13	1.9	0.1

Table II.2. Uniform residual stress evaluation coefficients

Rosette Type A Blind Hole Depth (mm)	$\bar{a}$	$\bar{b}$
0.0	0.000	0.000
0.1	0.013	0.024
0.2	0.031	0.058
0.3	0.051	0.096
0.4	0.072	0.136
0.5	0.090	0.176
0.6	0.108	0.213
0.7	0.122	0.248
0.8	0.135	0.279
0.9	0.145	0.305
1.0	0.152	0.329

*D_0 = 1.9 mm

Appendix III. Residual stress test results

Table III.1. Residual stresses calculation results

Location	Connection	$\sigma_{rs,p}$ (MPa)	$\sigma_{rs,min}$ (MPa)	β (degree)	$\sigma_{rs,long}$ (MPa)	$\sigma_{rs,tran}$ (MPa)	τ_{xy} (MPa)
1	X-0.5	355.48	143.78	-75.65	156.78	342.48	50.82
2		218.95	134.99	-25.84	203.00	150.94	-32.93
3		286.83	108.25	13.35	277.30	117.77	-40.12
4		326.61	190.03	5.97	325.14	191.51	-14.12
5		122.63	64.20	-2.29	122.54	64.29	2.33
6		118.87	-31.34	26.23	89.52	-1.99	-59.56
7		175.17	-28.85	39.73	91.80	54.52	-100.29
8		286.93	35.06	55.21	117.07	204.92	-118.03
9		216.97	48.71	-18.99	199.16	66.52	51.77
10		361.59	248.52	25.36	340.85	269.26	-43.76
11		384.88	270.19	32.43	351.90	303.17	-51.92
12		246.67	77.30	16.58	232.88	91.09	-46.32
1	X-0.7	456.56	90.50	-55.90	205.58	341.48	169.95
2		128.03	117.39	12.48	127.54	117.89	2.25
3		436.53	-18.29	-6.21	431.21	-12.96	48.91
4		327.94	235.84	69.25	247.40	316.38	-30.51
5		147.05	85.25	-12.92	143.97	88.34	13.46
6		368.23	-50.50	7.52	361.05	-43.33	-54.35
7		436.14	59.27	34.88	312.88	182.53	-176.81
8		273.83	-5.89	76.46	9.44	258.50	-63.66
9		273.69	101.34	25.53	241.68	133.34	-67.02
10		227.99	102.75	60.73	132.69	198.04	-53.42
11		267.52	121.52	-47.15	189.04	200.00	72.79
12		199.83	123.39	-13.87	195.44	127.78	17.79
1	GX-0.5	160.21	37.97	-56.80	74.62	123.55	56.01
2		109.47	58.60	-38.31	89.92	78.15	24.74
3		106.76	42.93	-6.85	105.85	43.84	7.56
4		125.37	70.30	-16.27	121.05	74.62	14.81
5		125.91	65.27	-17.89	120.19	70.99	17.73
6		150.17	43.54	24.21	132.24	61.48	-39.89
7		108.60	60.72	45.38	84.34	84.98	-23.94
8		124.99	39.24	53.88	69.03	95.20	-40.83
9		121.06	55.33	-4.97	120.57	55.83	5.67
10		145.28	62.83	43.72	105.89	102.21	-41.18
11		167.74	152.43	-45.93	159.84	160.33	7.65
12		140.04	66.54	12.07	136.82	69.75	-15.03

Location	Connection	$\sigma_{rs,p}$ (MPa)	$\sigma_{rs,min}$ (MPa)	β (degree)	$\sigma_{rs,long}$ (MPa)	$\sigma_{rs,tran}$ (MPa)	τ_{xy} (MPa)
1	GX-0.7	152.02	27.66	-70.84	41.05	138.63	38.55
2		177.98	33.37	-44.77	106.27	105.09	72.30
3		107.65	44.21	8.53	106.26	45.60	-9.30
4		132.17	69.00	20.00	127.31	82.18	-15.59
5		333.04	250.88	-34.82	306.25	277.67	38.51
6		146.19	49.39	23.49	130.81	64.76	-35.38
7		153.11	-13.73	63.46	19.58	119.81	-66.69
8		94.49	-30.00	-83.40	-28.35	92.84	14.21
9		101.36	67.93	-5.32	101.08	68.22	3.08
10		133.89	115.29	4.38	133.79	115.40	-1.42
11		267.02	165.94	-27.51	245.46	187.51	41.41
12		85.22	41.07	7.75	84.41	41.87	-5.89

Table III.2. Residual stresses perpendicular to weld toes

Connection	Residual Stress											
	$\sigma_{rs,1,90}$	$\sigma_{rs,2,45}$	$\sigma_{rs,3,0}$	$\sigma_{rs,6,0}$	$\sigma_{rs,7,45}$	$\sigma_{rs,8,90}$	$\sigma_{rs,9,90}$	$\sigma_{rs,9,45}$	$\sigma_{rs,9,0}$	$\sigma_{rs,12,0}$	$\sigma_{rs,12,45}$	$\sigma_{rs,12,90}$
X-0.5	342.48	209.90	277.30	89.52	173.45	204.92	66.52	184.61	199.16	232.88	208.31	91.09
X-0.7	341.48	124.96	431.21	361.05	424.51	258.50	133.34	254.53	241.68	195.44	179.40	127.78
GX-0.5	123.55	108.78	105.85	132.24	108.60	95.20	55.83	93.86	120.57	136.82	118.32	69.75
GX-0.7	138.63	177.98	106.26	130.81	136.38	92.84	68.22	87.73	101.08	84.41	69.04	41.87

Appendix IV. References

[1] M. Sun, J.A. Packer, Hot-dip galvanizing of cold-formed steel hollow sections: a state-of-the-art review. Frontiers of Structural and Civil Engineering 13 (2019) 49–65.

[2] G. Shi, X. Jiang, W. Zhou, T.M. Chan, Y. Zhang, Experimental investigation and modeling on residual stress of welded steel circular tubes. International Journal of Steel Structures 13 (2013) 495–508.

[3] R. Nasouri, K. Nguyen, A. Montoya, A. Matamoros, C. Bennett, J. Li, Simulating the hot dip galvanizing process of high mast illumination poles. Part I: Finite element model development. Journal of Constructional Steel Research 162 (2019) 105705.

[4] R. Nasouri, K. Nguyen, A. Montoya, A. Matamoros, C. Bennett, J. Li, Simulating the hot dip galvanizing process of high mast illumination poles. Part II: Effects of geometrical properties and galvanizing practices. Journal of Constructional Steel Research 159 (2019) 584-597.

[5] M. Sun, Z. Ma, Effects of heat-treatment and hot-dip galvanizing on mechanical properties of RHS. Journal of Constructional Steel Research 153 (2019) 603–617.

[6] K. Tayyebi, M. Sun, Stub column behaviour of heat-treated and galvanized RHS manufactured by different methods. Journal of Constructional Steel Research 166 (2020) 105910.

[7] K. Tayyebi, M. Sun, K. Karimi, Residual stresses of heat-treated and hot-dip galvanized RHS cold-formed by different methods. Journal of Constructional Steel Research 169 (2020) 106071.

[8] K. Tayyebi, M. Sun, Design of direct-formed square and rectangular hollow section stub columns. Journal of Constructional Steel Research 178 (2021) 106499.

[9] K. Tayyebi, M. Sun, K. Karimi, R. Daxton, B. Rossi, Experimental investigation of direct-formed square and rectangular hollow section beams. Journal of Constructional Steel Research 186 (2021) 106898

[10] K. Tayyebi, M. Sun, K. Karimi, R. Daxton, B. Rossi, Design of direct-formed square and rectangular hollow section beams. Journal of Constructional Steel Research 188 (2022) 107005

[11] ASTM, Standard specification for cold-formed welded carbon steel hollow structural sections (HSS), ASTM A1085/A1085M-15. American Society for Testing and Materials, West Conshohocken, PA, USA, 2015.

[12] CSA, General requirements for rolled or welded structural quality steel / Structural quality steel, CSA G40.20-13/G40.21-13. Canadian Standards Association, Toronto, Canada, 2013.

[13] C.K. Lee, S.P. Chiew, J. Jiang, Residual stress of high strength steel box T-joints Part 1: Experimental study. Journal of Constructional Steel Research 93 (2014) 20-31.

[14] C. Acevedo, A. Nussbumer, Influence of welding residual stress on stable crack growth in tubular K-joints under compressive fatigue loading, 13th International Symposium on Tubular Structures, Hong Kong: CRC Press/Balkema, Taylor & Francis Group (2010) 557-565.

[15] L. Tong, G. Hou, Y. Chen, F. Zhou, K. Shen, A. Yang, Experimental investigation on longitudinal residual stresses for cold-formed thick-walled square hollow sections. Journal of Constructional Steel Research 73 (2012) 105–116.

[16] Y.B. Wang, G.Q. Li, S.W. Chen, The assessment of residual stress in welded high strength steel box sections. Journal of Constructional Steel Research 76 (2012) 93-99.

[17] M. Sun, J.A. Packer, Direct-formed and continuous-formed rectangular hollow sections – comparison of static properties. Journal of Constructional Steel Research 92 (2014) 67-78.

[18] M. Sun, J.A. Packer, High strain rate behaviour of cold-formed rectangular hollow sections. Engineering Structures 62-63 (2014) 181-192.

[19] M. Sun, J.A. Packer, Charpy V-notch impact toughness of cold-formed rectangular hollow sections. Journal of Constructional Steel Research 97 (2014) 114-126.

[20] CSA, Limit States Design in Structural Steel, CSA S16-19, Canadian Standard association, Toronto, ON, Canada, 2019.

[21] X.L. Zhao, S. Herion, J.A. Packer, R.S. Puthli, G. Sedlacek, J. Wardenier, K. Weynand, A.M. van Wingerde, N.F. Yeomans, Design Guide for Circular and Rectangular Hollow Section Welded Joints under Fatigue Loading, CIDECT Design Guide No. 8, CIDECT and Verlag TÜV Rheinland GmbH, Köln, Germany, 2001.

[22] CSA, Welded steel construction, W59-18. Canadian Standards Association, Toronto, Canada, 2018.

[23] L.W. Tong, G.W. Xu, D.L. Yang, F.R. Mashiri, X.L. Zhao, Stress concentration factors in CHS-CFSHS T-joints: experiments, FE analysis and formulae. Engineering Structures 151 (2017) 406-421.

[24] R. Feng, B. Young, Stress concentration factors of cold-formed stainless steel tubular X-joints. Journal of Constructional Steel Research 91 (2013) 26-41.

[25] S. Daneshvar, M. Sun, K. Tousignant, Stress concentration factors for RHS-to-RHS X-connections near an open chord end. Journal of Constructional Steel Research 175 (2020) 106352.

[26] A. Ziaei Nejad, M. Sun, K. Tousignant, Circular hollow section X-connections near an open chord end: stress concentration factors. Journal of Constructional Steel Research 177 (2021) 106454.

[27] M. Sun, K. Tousignant, A. Ziaei Nejad, S. Daneshvar, Chord-end RHS-to-RHS and CHS-to-CHS X-connections with cap plates: stress concentration factors. Journal of Constructional Steel Research 179 (2021) 106567.

[28] ASTM, Standard test methods and definitions for mechanical testing of steel products, ASTM A370-17. American Society for Testing and Materials, West Conshohocken, PA, USA, 2017.

[29] ASTM, Standard test method for determining residual stresses by the hole-drilling strain-gauge method, ASTM E837-20. American Society for Testing and Materials, West Conshohocken, PA, USA, 2020.

[30] CEN, Eurocode 3: Design of steel structures – Part 1.9: fatigue, EN 1993-1-9:2005. European Committee for Standardization, Brussels, Belgium, 2005.

[31] J.L. Ma, T.M. Chan, B. Young, Material properties and residual stresses of cold-formed high strength steel hollow sections. Journal of Constructional Steel Research 109 (2015) 152–165.

[32] AWS, Structural welding code-steel, ANSI-AWS D1.1/D1.1M:2020. American Welding Society, Miami, USA, 2020.

[33] API, Recommended practice for planning, designing and constructing fixed offshore platforms – working stress design, API-PR2A-WSD. American Petroleum Institute, Dallas, USA, 2014.

[34] J. Jiang, C.K. Lee, S.P. Chiew, Residual stress and stress concentration effect of high strength steel built-up box T-joints. Journal of Constructional Steel Research 105 (2015) 164-173.

[35] Packer, J.A., Wardenier, J., Zhao, X.L., van der Vegte, G.J. and Kurobane, Y., Design guide for rectangular hollow section (RHS) joints under predominantly static loading, CIDECT Design Guide No. 3, 2nd. ed., CIDECT, Geneva, Switzerland, 2009.